buildings

MDPI

Article

A Study on the Optimization of Wind Environment of Existing Villa Buildings in Lingnan Area: A Case Study of Jiangmen's "Yunshan Poetic" Moon Island Houses

Zhaoming Du [1,*], Weihong Guo [2,*], Weicong Li [3] and Xuyi Gao [4]

[1] School of Architecture, South China University of Technology, Guangzhou 510641, China
[2] Architectural Design & Research Institute Co., Ltd., South China University of Technology, Guangzhou 510641, China
[3] Faculty of Built Environment and Surveying, Universiti Teknologi Malaysia, Johor Bahru 81310, Malaysia
[4] School of Art and Design, Guangdong Baiyun University, Guangzhou 510450, China
* Correspondence: zhaomingdu@outlook.com (Z.D.); whguo@scut.edu.cn (W.G.); Tel.:+86-139-2888-9298 (Z.D.)

Abstract: Effective natural ventilation reduces humidity, cools the space, and enhances thermal comfort. In light of the frequent ventilation issues in the Lingnan area, this research suggests a successful ventilation technique using Jiangmen's "Yunshan Poetic" Moon Island houses as an example. With its symmetrical architectural layout of townhouses and its primary courtyard villa product, the community typifies the Lingnan area. First off, we discovered that the district's average temperature is as high as 30.95 °C and its average humidity is as high as 83.592%RH using actual measurements and simulation of heat and humidity data. The district's buildings' issues with dampness, peeling walls, and substance mold are primarily caused by poor ventilation. Secondly, the PHOENICS program was used to provide efficient ventilation solutions for the following six aspects: external wind infusion organization, group orientation layout, planar grouping optimization, building façade combination, monolithic building openings, and indoor ventilation block. In order to determine if the technique is effective, the ventilation variables are compared before and after optimization using the Building Ventilation Effectiveness Test and Evaluation Criteria. The study concluded that the building's architectural characteristics and the local climate have an impact on natural ventilation's effectiveness. This serves as a guide for both the scientific layout development of future urban settlements and the optimization of ventilation of existing villa buildings in humid and hot areas.

Keywords: humid and hot area; villa building; wind environment; design strategy

Citation: Du, Z.; Guo, W.; Li, W.; Gao, X. A Study on the Optimization of Wind Environment of Existing Villa Buildings in Lingnan Area: A Case Study of Jiangmen's "Yunshan Poetic" Moon Island Houses. *Buildings* **2022**, *12*, 1304. https://doi.org/10.3390/buildings12091304

Academic Editors: S.A. Edalatpanah and Xi Chen

Received: 13 July 2022
Accepted: 19 August 2022
Published: 25 August 2022

1. Introduction

Over the past 40 years of reform and opening up, China's real estate industry has developed extremely rapidly [1]. During the period of 1997–2017, China's annual new urban population was close to 20 million people, bringing at least 5.2 billion square meters of housing demand, amounting to about 12 billion square meters of housing development area. It is also seen that Guangdong is currently the largest city in the country in terms of electricity consumption [2], with energy consumption of HVAC (heating, ventilation, and air conditioning) systems exceeding 40% of total household electricity consumption [3]; on the other hand, existing buildings developed by real estate developers generally have excessive energy consumption problems, with almost 68% of energy used for heating, ventilation, and air conditioning systems [4], accelerating the heat island effect [5] and forming a vicious circle. Although the real estate industry is an important guarantee for the GDP (Gross Domestic Product) growth of each local government [6], the future development goal should be to achieve a healthy habitat and economic sustainability simultaneously. Natural ventilation is the basic condition to guarantee a healthy living environment. Internationally, as early as the Rio de Janeiro Summit in Brazil in 1992, the use of wind heat and other natural resources to obtain thermal comfort and achieve energy saving and emission reduction has been agreed upon by the industry and has achieved results one after another, such as Stabile [7], Malkawi [8], Omrani [9], Masoumi [10], and other scholars, and some of these technologies have been successfully applied to building energy efficiency examples [11,12]. In China, most of the research has been based on HVAC systems for many years, but in 2011, academician Jiang Yi proposed the importance of building forms for energy saving and emission reduction [13]; in 2016, academician Cui Kai proposed the trinity of "technology–evaluation–architecture design" for green building design [14], which shifted the focus of China's green building "technology" to "method". Based on the above background, this study is an adaptive strategy research based on the current architectural design codes in China and the microclimate characteristics of the environment in which the research object is located.

The current state of research is for humid and hot regions. Victor Olgyay [15] (1963), the pioneer of the "bioclimatic localism" design theory, proposed the use of lighter building forms for natural ventilation design in humid regions and the adaptation of the design to the local climate, which had a profound impact on the architectural practice in humid regions such as Sri Lanka, India, and Malaysia. The Mahaweli Building, designed by Eoffrey Bawa in Sri Lanka in 1976, has an open design and uses canopies for shading and lake cooling to effectively solve the problem of building overheating in the local rainy and dry seasons. Charles Correa [16] (1980), India, proposed the design methodology of "form follows climate", which illustrates the influence of natural and unnatural environmental factors on the integration of resources such as hot-air paths in buildings, and provides a solution to the ventilation problems of buildings in hot and humid regions [17]. Kenneth King Mun Yeang, Malaysia, has influenced designers in Southeast Asia by focusing on the application of natural ventilation techniques such as double-skin façades, roof gardens, and atrium designs for high-rise buildings for many years.

As for the Lingnan region, Xia Changshi first proposed a "cooling strategy" for subtropical architecture in 1959 [18], which aroused the attention and research of Lingnan scholars on the inheritance of local ecological wisdom. In terms of building orientation, academician Mo Boji [19] (1959) proposed that the southeast orientation is the best orientation for Lingnan buildings to obtain good ventilation. With the advancement of simulation technology, this view was verified by later generations through quantitative studies by the end of the twentieth century; Lin Qibiao [20] (1997) further proposed that the best orientation for Lingnan buildings should cater to the dominant summer wind direction (157.5°) in Guangzhou. It is worth mentioning that as early as 2002, foreign scholar Gideon S. Golang [21] had clearly pointed out that the best orientation choice for buildings in Lingnan is southward, within 30° east of south, or within 15° west of south, in that order. In terms of architectural layout, Xia Changshi, Mo Boji, and She Junnan concluded in their early practice that the combination of Lingnan architecture and gardens plays an important role in microclimate regulation [22]. Taiwanese scholar Lin Xiande [23] (1996) argued that the staggered layout of buildings is more conducive to building ventilation, while Gao Yunfei [24] (2003) further pointed out through quantitative data that the effect of wind shadow zone on ventilation can be reduced when the building spacing is 0.7–1.1 times greater in staggered layout. Xie Hao [25] (2007) confirmed the effect of natural and artificial environmental forms on airflow. In 2016, Huixing Yu [26] concluded through simulation that good ventilation can be obtained under the dual effect of canyon effect and thermal pressure ventilation when the building aisles are designed in relative or staggered positions, which verifies the view of "climate space" proposed by Xiao Yiqiang [27] (2015). In terms of building morphology, the spatial scale of buildings affecting airflow has been paid attention to by domestic scholars, and Mo Bozhi [19] proposed ventilation optimization methods for interior spaces less than 9 m deep at an early stage. Later, Lin Qibiao [20] (1997) proposed a ventilation strategy in which the spacing between the back row and the front row of buildings is at least 1~1.2 times the height of the front building. On the basis of this, Song De-Xuan [28] (2003) further elaborated the possible impact of the front and rear rows of buildings on the ventilation of buildings in the wind shadow area due to the excessive height difference; Mai Hua [29] (2016) concluded through fluid dynamics analysis that the face width and height of buildings are proportional to the ventilation resistance of the building surroundings. In terms of ventilation openings, Zeng Zhihui [30] (2010) proposed a systematic ventilation combination strategy of "front wall opening–cold alley–patio" through actual measurements, and An-Shik Yang [31] (2014) suggested that opening high windows and door openings at a certain distance modulus could create temperature differences and wind-pulling effects in suitable seasons, which verified Zeng Zhihui's proposed strategy. Fang Pengfei [32] (2018) simulated the natural ventilation effect of 16 different exterior window forms under 19 working conditions, and concluded that the location of building vents has a significant effect on the airflow distribution of the indoor wind field. In terms of building window openings, the study showed that window-opening area and angle are directly related to indoor ventilation efficiency, and under the same conditions, Xia Yun [33] (2001) concluded that the ventilation effect of using single and grille windows is better than double windows, while the ventilation effect of upper- and lower-hung windows is positively correlated with an increase in opening angle.

The research on architectural design for climate adaptation in subtropical regions is early, has more achievements, and has gradually played a role in the level of energy saving in this region. In Lingnan, the research results on the passive ventilation wisdom of traditional buildings are richer, but the application of wind environment strategy based on simulation technology in contemporary architectural design is still in the initial stage; there is still a lack of systematic research, and the scientific utilization of wind environments in residential villa buildings has not been paid enough attention to, especially in terms of driving factors of the physical parameters of the building (building form) on the microclimate environment (influencing ventilation). The usefulness of appropriate building shapes for promoting natural ventilation is presumptively shown to be effective in this work and adds to existing research in the field through an experimental process of comparison, trial and error, and gradual improvement.

This study looks at how physical aspects of buildings might enhance natural ventilation in already-existing villa structures in hot and humid climates. The existing villa is a common housing type in Lingnan, which is a result of the demand for high-quality housing development in recent decades, is a problematic building in the urbanization process, and has high research value. Enhancing the natural ventilation performance of these structures benefits the settlement's environmental wellbeing, increases building energy efficiency, and offers design ideas for remodels, additions, and new villa structures. Initially, this article examines the actual issues and root causes of inadequate ventilation in the residential area, utilizing ENVI-NET models and measurements of the humid and warm environment. Second, ventilation is simulated using the PHOENICS program to investigate architectural approaches that can enhance natural ventilation in six different ways: external wind infusion organization, group orientation layout, planar grouping optimization, building façade combination, monolithic building openings, and indoor ventilation block. Finally, Stata statistics and a comparison of ventilation variables before and after the remodeling are used to demonstrate the success of the solutions.

2. Actual Measurement Method and Data Analysis

On-site measurement is a reliable method to assess the real condition of residential buildings [34]. The team adopts the method of "typical sample test + software simulation" to ensure the objectivity of data analysis, and starts from three levels: heat and humidity environment test, heat island intensity simulation, and natural ventilation state analysis. In contrast to the analysis of the heat and humidity environment, where the APMV evaluation indexes were obtained by converting the measured data and formulas, the other two levels of analysis were obtained by simulation using ENVI-MET software.

2.1. Research Subjects

This paper takes the "Yunshan Poetic" Moon Island Villa Settlement in Heshan City, Jiangmen, Guangdong Province, as an example (Table 1). The settlement, as a whole, faces north and south, with a comb-style layout and a symmetrical combination of townhouses and mirrors in combination with the road network, with most groups consisting of eight house types. Currently, the settlement provides five single-villa house types for users to choose from; each villa is two-story in scale, with independent courtyards and gable corridors encircling along three sides and connecting each room, reflecting the typical Lingnan traditional courtyard characteristics. The settlement was developed with the hope of making full use of the traditional cold-alley layout for ventilation and cooling purposes, and is a landmark residential project in Heshan for the integrated application of green building technology.

Table 1. Profile of the Moon Island Residence.

<table>
<tr><th colspan="2">Project Introduction</th><th colspan="2">Scene Photos</th><th colspan="2">Construction Group</th><th colspan="2">Building Units</th></tr>
<tr><td colspan="2">Villa name: "Yunshan Poetic"
Architectural style: New Chinese style
Building Type: Courtyard Villa
Location: Renmin East Road, Heshan, Jiangmen
Grouping Form: Row layout, mirror symmetry</td><td colspan="2"></td><td colspan="2">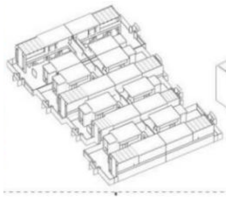</td><td colspan="2">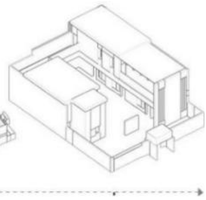</td></tr>
<tr><th colspan="5">A plan of the Moon Island Residence</th><th colspan="3">Huxing group form</th></tr>
<tr><td colspan="5"></td><td colspan="3"></td></tr>
<tr><th>The first floor</th><th>The second floor</th><th colspan="6">The ventilation of the villa</th></tr>
<tr><td></td><td></td><td colspan="2">
Damp wall peeling</td><td colspan="2">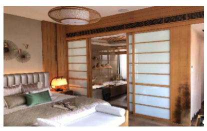
Material moldy and blackened</td><td>
Wallpaper crumpling and warping</td><td>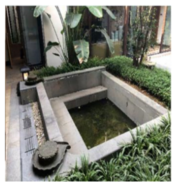
Insects and bacteria breeding</td></tr>
</table>

However, through field research, it was found that in less than a year after the completion of the community, the indoor and outdoor model villas had suffered from peeling walls, moldy decorative materials, crumpled and cracked wallpaper, and serious mosquito breeding, especially in the hot summer months from July to September, when the relevant problems are more prominent. To dig deeper into the root cause of the problem, the team conducted comprehensive heat and humidity environment measurements as well as a simulation.

A typical day of the early summer, 25 May, was chosen as the measurement date. It may be assumed that the building will remain hot throughout the summer if the heat and humidity environment of the homes in the Moon Island district does not match the national standard at the start of the summer.

2.2. Heat and Humidity Environment: Actual Measurement

The team chose the 157 m^2 house in the district with the best natural ventilation as the representative of the actual measurement because the actual measurement could not cover all villas in the area. Our team then used professional measurement equipment (Table 2) and set up enough measurement points to cover all functional areas to obtain the heat and humidity environment index (Table 3). The choice was made based on whether the following three criteria are met: (1) The building is in the front row on the side of the main wind direction; (2) there are no evident obstructions in the immediate vicinity; (3) the outside wind speed is smooth; and (4) the household type is the most prevalent household type in the area. The house also suffers from the same heat and humidity environment problems mentioned earlier.

Table 2. Measurement equipment introduction.

Monitoring Parameters	Instrument Name	Instrument Range	Instrument Precision	Instrument Photograph
v (m/s) Wind direction (°) atm (hPa) t_{out} (°C) RH_{out} (%)	BX portable weather station	0~70.0 m/s 0~360° 10 hPa~1100 hPa −50 °C ∼ 60 °C 0~100%	±0.3 m/s ±1° ±0.1 hPa ±0.3 °C ±3%	
t_{in} (°C) RH_{in} (%) v_a (m/s)	TES-1341 anemometers	−10 °C~60 °C 0~100% 0~30.0 m/s	±0.1 °C ±3% ±0.01 m/s	
t_g (°C)	JTR04 black-bulb thermometers	−20 °C~125 °C	±0.5 °C	

Table 3. Overview of the actual test.

<table>
<tr><th colspan="5">Actual Measurement Deployment</th></tr>
<tr><td></td><td></td><td>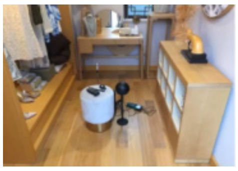</td><td></td><td></td></tr>
<tr><td>guest bedroom</td><td>Bathroom</td><td>Master bedroom</td><td>Cloakroom</td><td>kitchen</td></tr>
<tr><th colspan="3">Measured working conditions</th><th colspan="2">Actual measurement results</th></tr>
<tr><td colspan="3" rowspan="2">measurement time: 25 May 2021, 19:00–26 May 19:00 (a day and night; 24 h continuous monitoring)
condition: 25 May 2021 19:00–22:00 (sunny), 22:00–the next day 06:00 (rain); 26 May 06:00 (sunny), 12:00–19:00 (cloudy)
Deployment points: 10
Deployment areas: Kitchen, living room, public bathroom, three bedrooms and bathroom, checkroom
Measuring height: 1.1 m from the ground</td><td colspan="2">Average wind speed: 0.18 m/s;
Dominant wind: Mainly south;
Temperature range: 25–32.6 °C</td></tr>
<tr><td colspan="2">Average temperature:27.7 °C;
Humidity range: 65.4–92%RH;
Average humidity: 83.592%RH</td></tr>
</table>

The data were collected by the related instruments (Table 2). For the thermal environment, the BX portable weather station was used to collect the outdoor air velocity (V), wind direction, atmospheric pressure (atm), air temperature (t_{out}), and humidity (RH_{out}) data. At the same time, data were collected using TES-1341 anemometers and JTR04 black-bulb thermometers in 10 rooms to record indoor air temperature (t_{in}), humidity (RH_{in}), air velocity (v_a), and 24 h black globe temperature (t_g), starting at 1:30 a.m. on 18 July 2019. Based on the Standard of Test Methods for Thermal Environment of Buildings, the data of RH_{in} and t_g were collected 0.6 m above the ground, while the data of t_{in} and v_a were collected 1.1 m above the ground.

The analysis of the heat and humidity environment is based on the engineering calculation method. The engineering calculation is based on the "Adapted Predicted Mean Vote (APMV) [35]", which is calculated by Equation (1), while the "Predicted Mean Vote (PMV)" is calculated by Equations (2)–(5) [36], where the average radiation temperature is calculated by Formula (6) [37] based on the measured data.

The APMV value can be obtained by Equation (1).

$$\mathrm{APMV} = \mathrm{PMV}/(1 + \lambda \cdot \mathrm{PMV}) \tag{1}$$

The PMV value can be obtained by Equation (2).

$$\begin{gathered}\mathrm{PMV} = \left[0.303 \times e^{-0.036M} + 0.028\right]\{M - W \\ -3.05 \times 10^{-3}[5733 - 6.99(M - W) - P_a] - 0.42 \\ [(M - W) - 58.15] - 1.7 \times 10^{-5}M(5867 - P_a) \\ -0.0014M(34 - t_a) - 3.96 \times 10^{-8} f_{cl} \cdot \left[(t_{cl} + 273)^4\right. \\ \left. -(\bar{t}_r + 273)^4\right] - f_{cl}h_c(t_{cl} - t_a)\Big\}\end{gathered} \tag{2}$$

The t_{cl} value can be obtained by Equation (3).

$$\begin{gathered}t_{cl} = 35.7 - 0.028(M - W) - I_{cl}\Big\{3.96 \times 10^{-8} f_{cl} \times \left[(t_{cl} + 273)^4 - \right. \\ \left.(\bar{t}_r + 273)^4\right] + f_{cl}h_c(t_{cl} - t_a)\Big\}\end{gathered} \tag{3}$$

The h_c value can be obtained by Equation (4).

$$h_c = \begin{cases} 2.38|t_{cl} - t_a|^{0.25} & \text{when } 2.38|t_{cl} - t_a|^{0.25} > 12.1\sqrt{v_{ar}} \\ 12.1\sqrt{v_{ar}} & \text{when } 2.38|t_{cl} - t_a|^{0.25} < 12.1\sqrt{v_{ar}} \end{cases} \quad (4)$$

The f_{cl} value can be obtained by Equation (5).

$$f_{cl} = \begin{cases} 1.00 + 1.290 I_{cl} & \text{when } I_{cl} \leqslant 0.078\ \mathrm{m^2 \cdot K/W} \\ 1.05 + 0.645 I_{cl} & \text{when } I_{cl} > 0.078\ \mathrm{m^2 \cdot K/W} \end{cases} \quad (5)$$

The $\bar{t}_r$ value can be obtained by the following Equation (6).

$$\bar{t}_r = \left[(t_g + 273)^4 + \frac{0.25 \times 10^8}{\varepsilon_g} \left(\frac{|t_g - t_a|}{D} \right)^{\frac{1}{4}} \times (t_g - t_a) \right]^{\frac{1}{4}} - 273 \quad (6)$$

where M is the metabolic rate, set to 58.15 $\mathrm{W/m^2}$ (sitting activity); W is the heat consumed by external doing work, set to 1.2 met (sitting activity); I_{cl} is the clothing thermal resistance, summer clothing thermal resistance is set to 0.5 clo (assuming wearing liner pants, short-sleeved shirts, light pants, thin shorts, shoes); f_{cl} is the ratio of human body surface area when dressed to human body surface area when naked; t_a is air temperature, set to 27.7 °C (measured); $\bar{t}_r$ is the mean radiant temperature; v_{ar} is the airflow velocity, set to 0.18 m/s (measured); P_a is the partial pressure of water vapor; h_c is the convective heat transfer coefficient $\mathrm{W/m^2 \cdot {}^\circ C}$; t_{cl} is the temperature indicated by the clothing; and adaptive coefficient λ is taken as 0.21 according to the specification. Complete formula and parameter values refer to national standards [36].

Finally, the calculated APMV values are plotted in a chart (Figure 1), and the standard of "evaluation of heat and humidity environment of non-artificial cold and heat sources" [38] is referred to (Table 4). When more than 90% of the main functional rooms or areas in the building meet the conditions of a certain evaluation level, it can be judged that the building reaches the corresponding level [39].

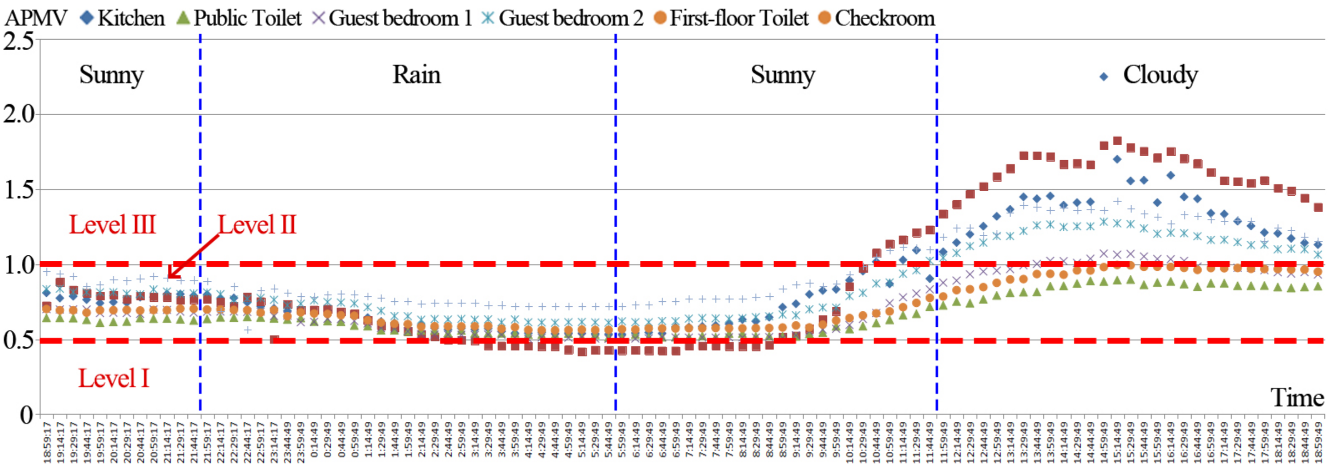

Figure 1. Hot and humid environment APMV change.

Table 4. Non-artificial heat- and cold-sourced heat and humidity environment evaluation index.

Level	Evaluation Criteria (APMV)
Level I	$-0.5 \leq \mathrm{APMV} \leq 0.5$
Level II	$-1 \leq \mathrm{APMV} < -0.5$ or $0.5 < \mathrm{APMV} \leq 1$
Level III	$\mathrm{APMV} < -1$ or $\mathrm{APMV} > 1$

Comprehensive actual measurement results and analysis of the data yielded (Table 5): From 19:00 to 22:00 on 25 May (sunny), the overall heat and humidity environment basically met the Level II index; from 22:00 to 6:00 on 25 May (rainy), it basically met the Level II index, and the living room reached the Level I index; from 6:00 to 12:00 on 26 May (sunny), the environment basically met the Level II index; from 12:00 to 19:00 (cloudy), due to the rising temperature at noon, only the two guest bedrooms and bathrooms on the first floor met the Level II index, and the rest of the rooms, as a whole, reached the Level III index. From the overall data, the thermal comfort of villas with the best natural ventilation basically met the Level II index, while some rooms and time periods only met the Level III index. It can be inferred that villas in the back row and villas in the leeward area with poor natural ventilation did not meet the Level III index to a large extent.

Table 5. APMV thermal and humid environment stages: actual test evaluation.

Monitoring Time	Monitoring Results
25 May, 19:00 to 22:00 (Sunny)	APMV values for all rooms were Level II.
25 May, 22:00 to 26, 6:00 (rain)	The rooms basically met the Level II indicators; the living room in the early morning reached the Level I indicators.
26 May, 6:00 to 12:00 (Sunny)	The measured rooms basically met the index of Level II; the temperature rose near noon, and APMV gradually increased
26 May, 12:00 to 19:00 (overcast)	As the temperature rose at noon, only the first two guest bedroom bathrooms met the Level II indicators, and the rest of the rooms, as a whole, met the Level III indicators

2.3. Heat Island Intensity Simulation

The heat island effect, when a region's temperature is greater than its surroundings, is a phenomenon and the heat island intensity is an indicator that measures its severity. The average heat island intensity reflects the average heat island effect of a region over a certain period of time. In this study, heat island intensity simulations were carried out using ENVI-MET, a software that simulates urban microclimates and is frequently utilized for meso-scale urban thermal environment investigations. The human body's reaction to thermal comfort, which varies depending on regional temperature differences, is its level of contentment with the objective thermal environment. The evaluation of thermal comfort can be referred to as the PMV index [40].

In order to truly reflect the outdoor summer microclimate characteristics of the Moon Island district, this simulation extracted the corresponding typical meteorological year data from the "China Building Thermal Environment Analysis Special Meteorological Data Set", station number 59,287, selected 7.22 as a typical summer day, set the dominant wind direction as south-southeast wind (SSE), and the average wind speed as 2.3 m/s. The geographic location of the model is 23.10° N, 113.20° E, and the East 8 CST/UTC+8, 120° E is adjusted as the reference time zone of the model. The simulation start time is 0:00, and the simulation duration is 24 h. The first 9 h is the simulation preheating time, so the data of the 9 a.m.–7 p.m. period are selected as valid data for analysis. The floor material is set to concrete, referring to the requirements of GB 50176-2016 "Thermal Design Code for Civil Buildings" (Table 6), and other parameters are the default values of the system.

Table 6. Ground parameter settings.

Surface Reflectance	Surface Emissivity	Constructed Composition (from Top to Bottom)	Thermal Conductivity/(W/m^2·K)	Volumetric Heat Capacity/(KJ/(m^3·K))
0.3	0.9	150 mm concrete	0.52	1274
		230 mm sand	0.58	1616
		Plain soil layer	0.93	1800

After simulation, the average heat island intensity index (Table 7) obtained for the Moon Island cell was evaluated with reference to the PMV index (Table 8). The results show that the community, as a whole, meets the national average daily heat island intensity standard (less than 1.5 °C) [41]; however, it exceeds this value during the period of 2:00–5:00 p.m., and the average temperature in the courtyard reaches 30.95 °C. The average temperature in the courtyard of the villa, sitting in the best natural ventilation conditions of the community, exceeds the average temperature of the Lingnan transition season (average temperature 20~25 °C) [42] 5.95 °C~10.95 °C, with an average heat island intensity of 1.02, and the site felt overheated physically.

Table 7. Cell average heat island intensity data simulation based on ENVI-MET.

Time Node	Outdoor Ambient Temperature (°C)	Outdoor Average Temperature (°C)	Heat Island Intensity (°C)
9:00	29.00	28.82	−0.18
10:00	29.70	29.56	−0.14
11:00	30.40	30.71	0.31
12:00	30.90	31.52	0.62
13:00	31.10	32.20	1.10
14:00	31.00	32.66	1.66
15:00	30.70	32.53	1.83
16:00	30.10	31.99	1.89
17:00	29.40	31.34	1.94
18:00	28.80	30.21	1.41
19:00	28.10	28.95	0.85
Average	29.93	30.95	1.02

Table 8. Indoor thermal comfort index for PMV in the range −1–+1.

Cold	Cool	Slightly Cooler	Thermal Comfort	Slightly Warmer	Warm	Heat
−3	−2	−1	0	1	2	3

2.4. Natural Ventilation Condition

Grasshopper is a plug-in that runs in the Rhino environment and uses procedural algorithms to generate models that are widely used to evaluate building performance. The year-round natural ventilation comfort of the courtyard is simulated using the Ladybug and Honeybee functions of the Grasshopper plug-in. Honeybee is a redevelopment of the Ladybug function, adding the performance of calculating adaptive thermal comfort. First, we imported the site model and the local 2022 EPW weather data file [43], checked the adaptive model for evaluation, set the calculation time period to year-round, set the wind speed value to 0.18 m/s (actual data), and used the ASHRAE standard and daily average calculation method for outdoor average temperature [44]. Secondly, the "simulation time step" was set to 6 times per hour, and the "solar radiation distribution calculation method" was set to "complete indoor–outdoor reflection" mode to obtain a more accurate representation. The "shading calculation method" is set to "pixel counting" to avoid the "non-convex hull" error of the model.

As a result of the simulation, the data on the percentage of time the room is in thermal comfort throughout the year under natural ventilation conditions (Table 9), as well as the indoor natural ventilation year-round thermal comfort status graphs for the first-floor living and dining room (Figure 2) and bedroom (Figure 3) were obtained. The output of the visualization chart is evaluated with the PMV index, and the specific values are displayed in red, yellow, and blue for hot, comfortable, and cold, respectively.

Table 9. The percentage of time the room is in thermal comfort throughout the year under natural ventilation conditions.

Name of the Room	Kitchen	Living and Dining Room	Bathroom	The Guest Bedroom on the First Floor A	The Guest Bedroom on the First Floor	Master Bedroom	Cloakroom
Year-round comfort time (%)	44.83	47.02	50.95	40.33	40.61	20.95	22.04

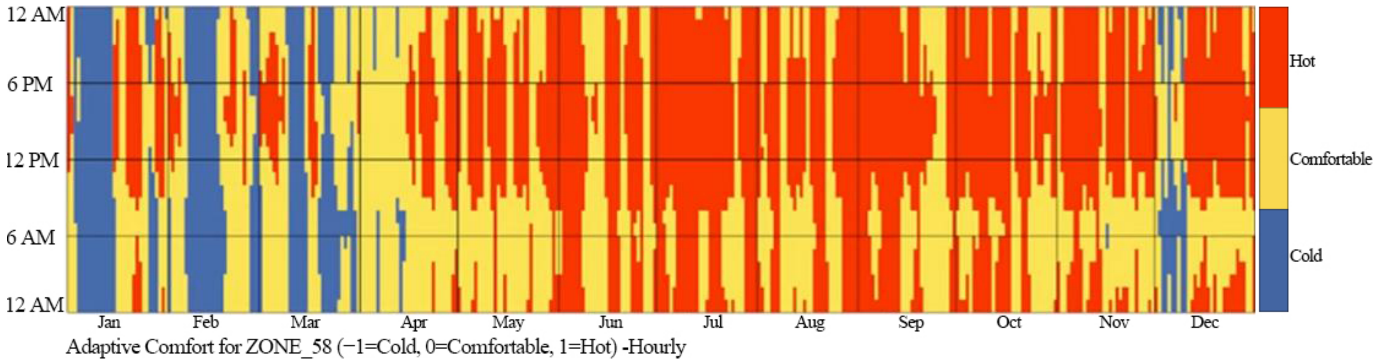

Figure 2. Natural ventilation state of the first-floor bedrooms in the year-round thermal comfort state diagram.

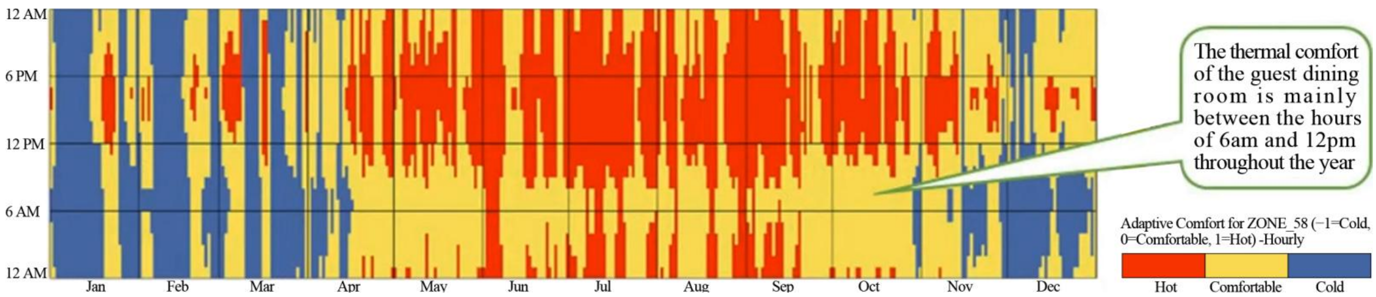

Figure 3. Natural ventilation state of the first-floor living and dining room with year-round thermal comfort state.

From the data, under the natural ventilation condition, the best indoor thermal comfort hours throughout the year are in the bathroom, followed by the second-floor living and dining room, kitchen, and two guest bedrooms, while the second-floor master bedroom and the checkroom lack good performance. Specifically, the year-round thermal comfort condition of natural ventilation in the first-floor living and dining room is mainly concentrated in the period from April to November, from 5:00 a.m. to 9:00 p.m. In the same period, from 10:00 a.m. to 8:00 p.m., the PMV value is >1 and the indoor temperature is warm and warm air is blowing. In contrast, the performance of the first-floor guest bedroom shows a distinctly uneven distribution and short duration throughout the year, with PMV values >1 from June to November; when the room is hotter and the whole day is extended, the end month is extended to December.

3. Wind Environment Optimization Strategy for Existing Villa Buildings in Lingnan Area

The actual measurement results showed that the average temperature in the district was as high as 30.95°, which exceeded the national standard value (20–25 °C), the average humidity reached 83.592%RH, which also far exceeded the national standard value (30–60%RH) [45], and poor ventilation was the main reason behind the heat and humidity collecting indoors. Building night ventilation is available to obtain a cooling effect [46], but the higher humidity during the day makes night ventilation unable to achieve the expected purpose [47]; therefore, improving ventilation throughout the day is an effective way to cool down and dehumidify in Lingnan. Therefore, in this paper, PHOENICS software, which is currently widely used by the industry, is selected for the optimization strategy analysis. This software provides a variety of turbulence models available for analysis, high compatibility with the analyzed models, and accurate data analysis. "Optimization" refers to an experimental process of comparison, trial and error, and incremental improvement.

3.1. Model Adjustment and Parameter Setting

PHOENICS is a software of computational fluid dynamics. We used the 2016 version of this software to simulate the ventilation. The data analysis of PHOENICS software starts from three steps of modeling, setting, and calculation. For the hot and humid climate of Lingnan, it is more meaningful to pay attention to its ventilation, heat dissipation, and dehumidification in summer rather than to its anti-freezing and wind-proofing in winter, so the meteorological parameters are taken in summer. Referring to the Civil Building Green Performance Calculation Standard JGJ/T 449-2018 Appendix B, the summer wind is set to SSE (south-southeast wind) with an average wind speed of 2.3 m/s. The AUTOCAD model with a high compatibility rate and low error tolerance is selected for the modeling stage to import and set parameters [48], the FLAIR module and finite volume method are selected for the calculation method [49], and the calculation domain is simulated according to the specification requirements (CJJ/T 309-2013, Standard for testing and evaluating the effect of building ventilation). The height is H, the distance from the inlet direction and the upper side to the simulated object is at least 5H, the outflow distance is at least 10H [50], and the blockage rate of the calculated cross section's size orthogonal to the mainstream direction is less than 3%. The wind velocity gradient distribution power index (α) is 0.16 according to the specification; the turbulence calculation model adopts the standard k-ε model suitable for near-earth wind simulation [51], and finally generates the grid and starts the calculation until the results converge [52].

According to the modeling analysis, the overall orientation of the settlement is in the shape of a "bar" of 17° NW, forming a wind angle of 22.5° with the summer wind of 157.5°; the summer wind is blocked by the southeast direction of Dayan Mountain, which will have a certain influence on the natural wind direction, and the overall wind outside the district is southerly (Figure 4), which is a key factor to be considered in the following. The wind direction of PHOENICS was adjusted to 175°, on the basis of the real data parameters, which formed an angle of 5° with the dominant wind direction (Figure 5), making the data more intuitive.

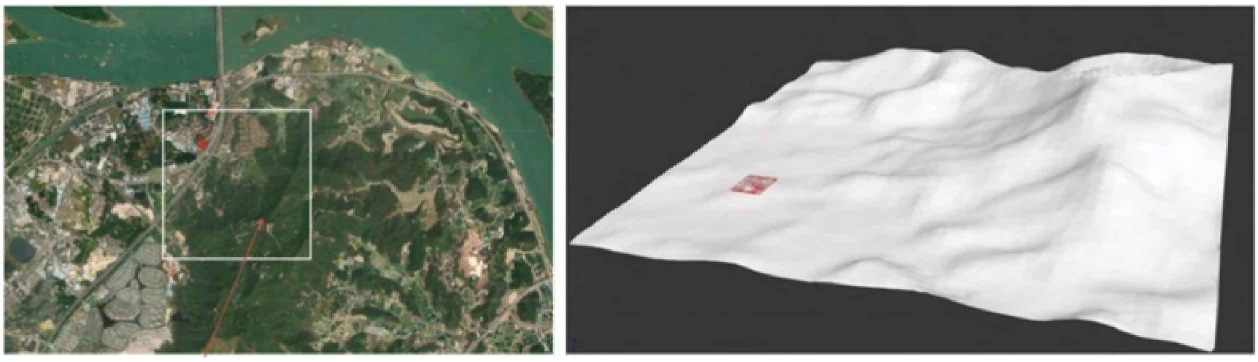

Figure 4. Summer winds are blocked by the southeasterly Great Wild Goose Mountains, with overall southerly winds.

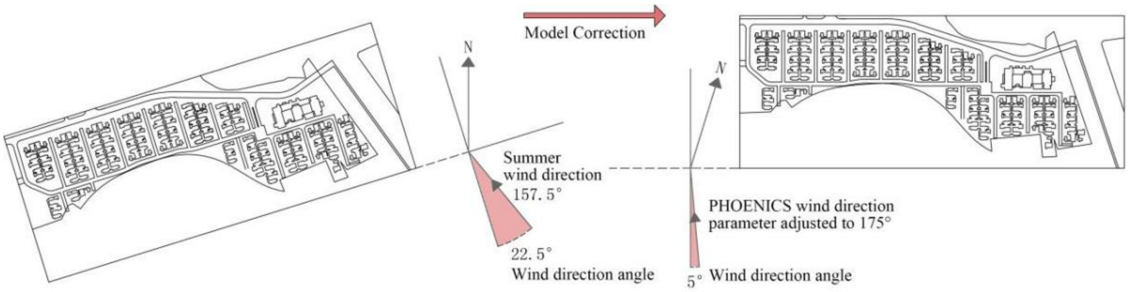

Figure 5. Schematic diagram of site simulation correction.

3.2. Wind Environment Optimization Design Strategy for Existing Villa Buildings in Lingnan Area

3.2.1. External Wind Infusion Organization

The external deflector component refers to the components that constitute the overall environment around the building and influence the gas flow, including vegetation, mountains and water, etc. Among them, the optimization of vegetation is the most direct way to promote the improvement of external wind in the local environment [53]. The tree belt (6 m) in the southern part of the settlement blocks most of the natural wind flow (Figure 6). The idea of optimizing it is to achieve natural ventilation for the low-rise buildings by adjusting the scale of the alleyways, controlling the density of the trees, and forming a staggered layout with the buildings and the street network, and then combining it with two or more openings on both sides of the villa building combination units to create cross-ventilation conditions and a higher ventilation rate [54]. With the same setting parameters, Figure 7 shows the simulation after adjusting the layout. the tree belt before optimization behaves as a wind wall to isolate the new air outside the community, and after optimization, the trees are divided into wind corridors, and the airflow is reorganized and balanced for both sides to enhance the wind flow rate.

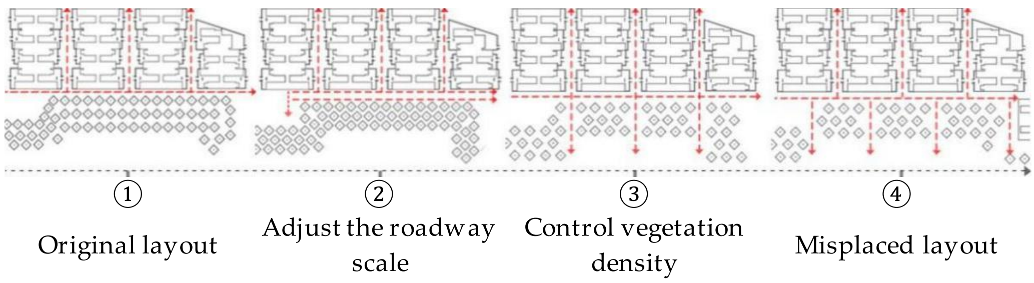

Figure 6. Optimization process of external wind flow organization.

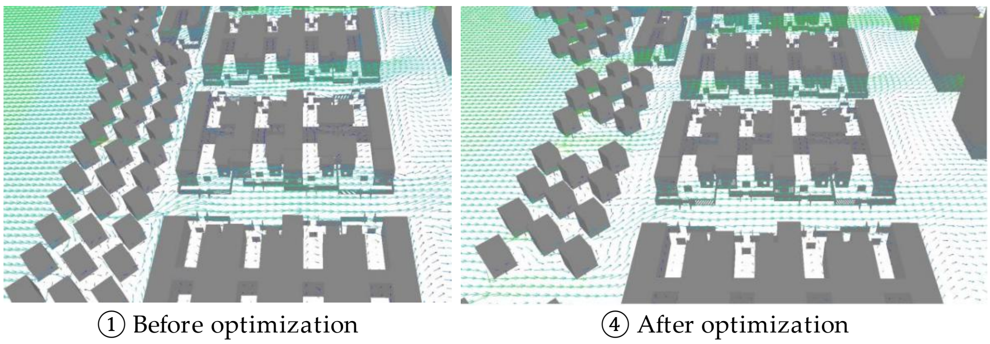

Figure 7. Wind direction diagram before and after optimization (Shows the flow path variation of ventilation).

3.2.2. Group Orientation Layout

Building orientation is considered to be one of the most effective passive methods to obtain natural ventilation in hot and humid regions [55]. The optimal orientation of buildings varies considerably between regions, even for the same climate conditions. For the same hot and humid climate, buildings facing north and south in Singapore are considered to have better indoor thermal comfort than buildings facing east and west [56], the optimal orientation range for buildings in Kuala Lumpur and Bangkok is considered to be between 150° and 188° (Between south-southeast and due south) [57]. Gideon S. Golany pointed out that the best choice of orientation for buildings in the Lingnan area is within 30° east of south or 15° west of south [21]. As mentioned above, the optimal orientation range for the humid and hot areas can be specified as a choice between south-southeast and 15° southwest.

However, Cheuk Ming Mak [58] believes that if the ventilation is considered from the angle of wind incidence and wall formation, when the wind angle forms 45°, the average wind speed in the room is larger and uniformly distributed, which is different from the above-mentioned scholars' views. In order to compare and verify the optimal orientation from these variabilities, four wind directions—the original layout (5° east of south), 15° west of south, due southeast, and due southwest—were selected for ventilation simulations in this paper under the condition of ensuring a consistent average wind speed (2.3 m/s) to compare the wind speed at a profile height of 1.5 m (Figure 8). The directions of due southeast and due southwest were chosen to further compare and verify the conclusions of the above scholars.

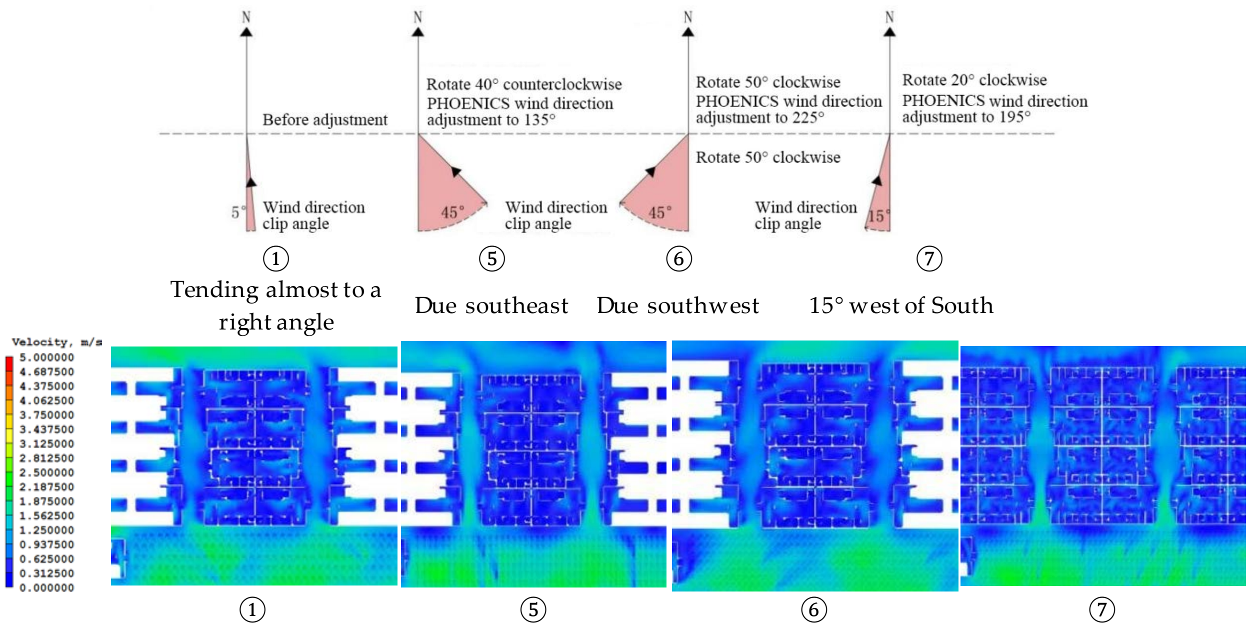

Figure 8. Process of community orientation optimization and simulation results.

Simulation shows (Figure 8) that the open courtyard gates of each villa in the original layout ① are almost parallel to the dominant wind direction, natural ventilation depends entirely on the wind fluctuation, the indoor wind field is more difficult to form, and there is a large area of static wind area in the courtyard and indoors. When the wind angle is due southeast ⑤ and due southwest ⑥, the courtyard entrance has a mass wind, but the persistence is insufficient, while when the wind angle is 15° west of south ⑦, the indoor changes little and the courtyard changes from a large static wind area to a quasi-static wind area. Therefore, it is proved in this simulation that 15° west of south is the best orientation for the building layout of the Moon Island community, which is consistent with the views of Qibiao Lin [20] and Gideon S. Graney [21].

3.2.3. Planar Grouping Optimization

The form of the building group is one of the main spatial elements affecting ventilation, and is often analyzed in detail using several morphological indicators [59] such as sky-view factor (SVF), street-height-to-width ratio, and block density. Vertically closed gaps, open porches [60], the combination of wide and narrow street changes [61], parallel courtyard layout, etc. have been proven to enhance ventilation and improve air quality [62], and there are also a number of studies that have proven that the street width and the ratio of the height of buildings on both sides of the street and the wind path have a certain regularity and are directly affected by the layout. The layout is divided into wind corridors by matrix separation, forming cold alleys, strengthening the airflow inside the block, and helping to take away the internal hot and humid airflow [63].

The Moon Island district mostly forms building clusters with mirror symmetry of eight households and distributes them in a row. Drawing on the above principles, the layout is reorganized (Figure 9) and the clusters are divided into the planar forms of one-character ventilation ⑧, cross ventilation ⑨, and matrix ventilation ⑩ to compare the influence of the morphology of internal air cavities on ventilation. In fact, the length, width, and height of the internal air cavity formed by the cold alley also affect the airflow variation [64], i.e., the formation of gyratory clustered wind in a small area. In this study, based on the matrix ventilation, the scale is appropriately adjusted to form the gap (⑪) that plays the role of the "canyon effect". The volume relationship of the building block organization affects the wind field effect generated by the overall morphological changes [65], and is correlated with the wind speed and direction in the wind field [66]. According to the rule of thumb for cross-ventilation, the building length (L) should be less than five times the building height (H) to produce effective indoor ventilation [67], i.e., when the building length is much larger than the building height, it can be adjusted to obtain the best ventilation. Drawing on this principle, the study used the dichotomy method based on matrix ventilation, splitting the eight-family combination into a small-volume row of four-family combinations and arranging them in a fishbone layout for simulation (⑫), while further comparing the ventilation effects of high-density longitudinal layout ⑬ and horizontal layout ⑭, considering the later developers' development needs for a greater number of residences.

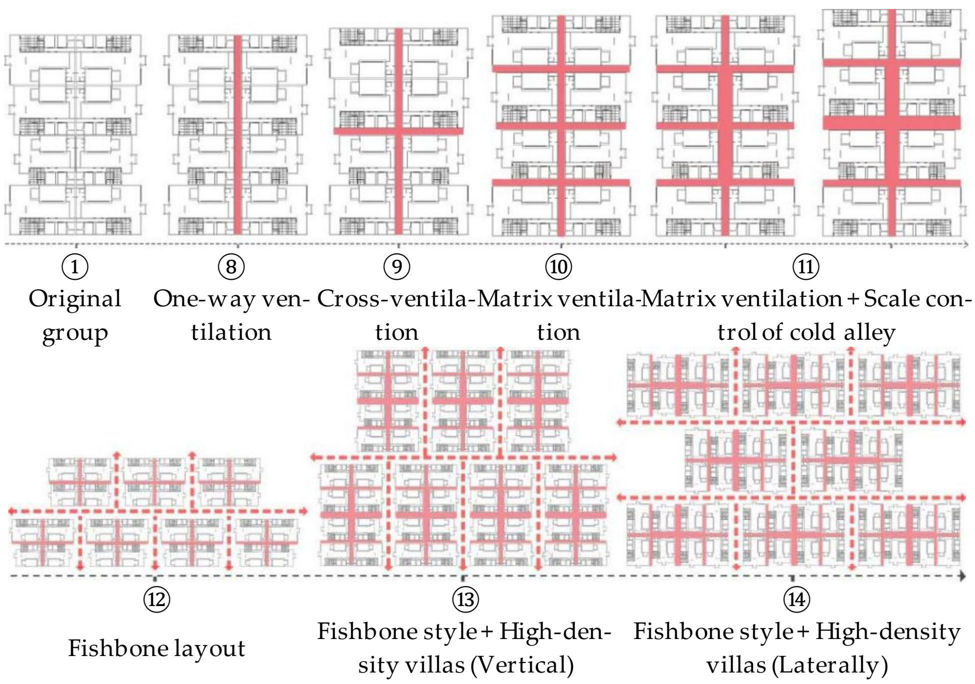

Figure 9. Planar grouping optimization process.

The simulation shows (Figure 10) that cluster ⑧ forms an internal wind cavity due to the narrow and long cold-alley breezeway, which accelerates the wind circulation, but the improvement of ventilation in the courtyard and indoors is not obvious. In contrast, the wind velocity of wind cavities in clusters ⑨ and ⑩ is weakened, and the wind velocity inside the courtyard is slightly improved, but the improvement inside is still not significant. In cluster ⑪, when the airflow enters from the open space to the narrow cold alley, the airflow is accelerated, and when it reaches the wide fork in the middle, the airflow is dispersed to all corners, although the wind speed will be reduced [68], and the turbulence inside the cold alley is richly varied, with more saturated ductile winds at the entrance of the courtyard and continuing to the center of the courtyard. It is worth mentioning that, compared with cluster ⑩, cluster ⑫ did not play an accelerating effect on wind speed because of the reduction of building mass and the change of layout from dense to sparse. In cluster ⑬, the ventilation of the rear-row buildings is not weakened by the change of the length of the front-row building group, and this result is somewhat different from the view of Ye Qing [65] and Liu Junnan [66]. Compared with cluster ⑬, the housing volume ratio of ⑭ is higher, but because the lateral scale of the back-row buildings' leeward area is wider, the cyclonic wind generated by the wind pressure on the windward and backward side cannot penetrate deeply into the central area of the building leeward area; the ventilation of the north-facing household type of the back-row buildings is poor, which confirms that the Moon Island district has certain disadvantages in terms of ventilation if it adopts a lateral layout, i.e., the building row orientation is almost at a right angle to the dominant wind direction. Therefore, if only the eight-family group is considered, the best ventilation effect is produced by using cluster ⑪ in Moon Island, and considering the future development of high-density villa products, the overall wind field effect of cluster ⑬ is better.

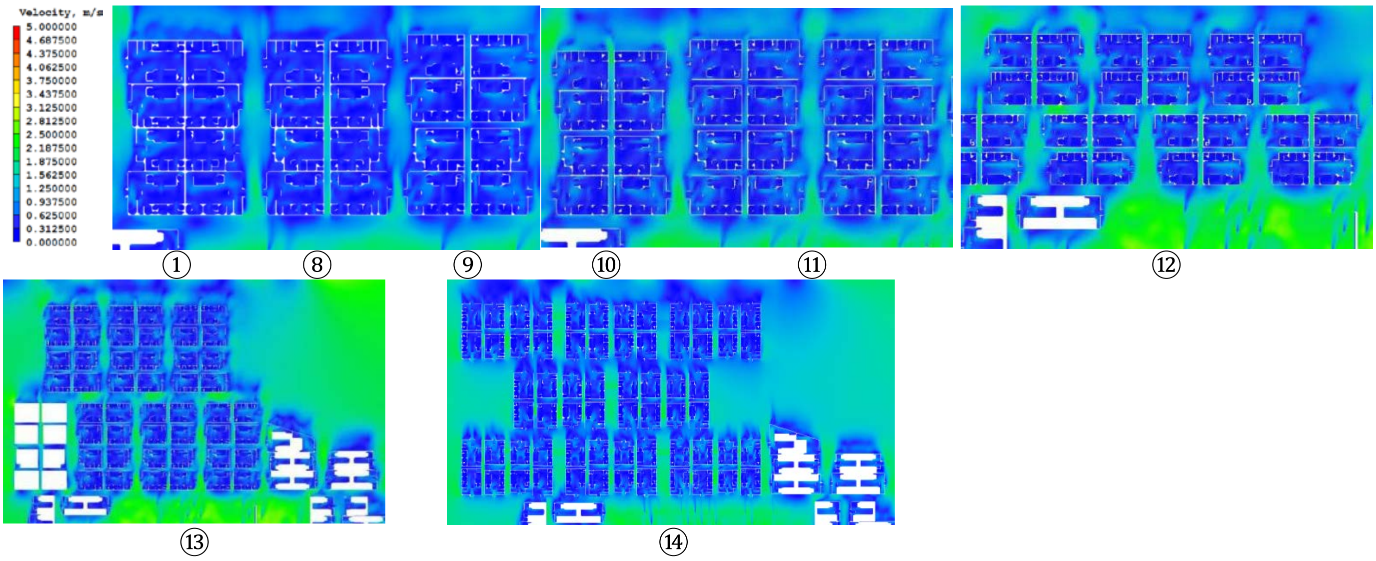

Figure 10. Simulation results of planar grouping optimization process.

3.2.4. Building Façade Combination

Some studies point out that the wind speed of the courtyard is directly proportional to the size of the courtyard and inversely proportional to the degree of courtyard enclosure and wall height [69]. Klote [70] points out that when the air inlet is as low as possible and the height of the building space is as large as possible, the better the ventilation superposition effect induced by the multi-block space design. It has also been suggested that unless more than half of the interfaces of a block are missing, the internal isolation of tall and narrow spaces is still stronger, while for low and open spaces, even if there are no gaps around them, the gas circulation of their internal environment is still stronger [71]. The above ideas reflect the role of object scale, undulation, and sparseness relationships on the wind. Liping, a Singaporean scholar, has also proposed façade design strategies that facilitate indoor ventilation and thermal comfort for the local climate [72]. Therefore, this study finds the best solution by comparing the ventilation effects of buildings with three elevation variations: parallel, stepped, and "treasure bowl".

Parallel façade means that the height of the front and rear rows of buildings tends to be the same. Stepped façade means that the height of the combined buildings has a change in height, and the back row of buildings is higher than the front row of buildings. Treasure bowl is a symmetrical layout of two-stepped combination buildings, which forms a height difference of "high on both sides and low in the middle" in the building façades.

According to the simulation (Figure 11), when the heights between the buildings are parallel to each other ⑮, the lack of a rich variation in height has less impact on the air pressure difference and does not produce better air circulation [34]. In the stepped façade, the change in the height level of the building will produce a difference in air pressure and a strong truncation of the wind direction, easily forming cyclonic wind through wind pressure differences to supplement the backwind area of the building, and the turbulence duration on the windward side increases as a result. Generally, the relationship between orientation of the building layout and the wind direction can produce a large wind pressure difference, which can create the best ventilation for the room [73], but may not be able to generate the best ventilation comfort [74]. In contrast, the treasure bowl ⑰ forms a hierarchy of height differences between the two sides and the middle, and the intersecting walls generate indoor air pressure, but due to the richness of the height differences in the adjacent buildings, the wind pressure value is weakened to a certain extent while creating the best ventilation, and the wind flowing around it is increased. The wind circulation in the concave space increases the chance of wind penetration into the courtyard and the interior, which can compensate, to a certain extent, for the poor ventilation of the rear buildings in the flat group ⑭.

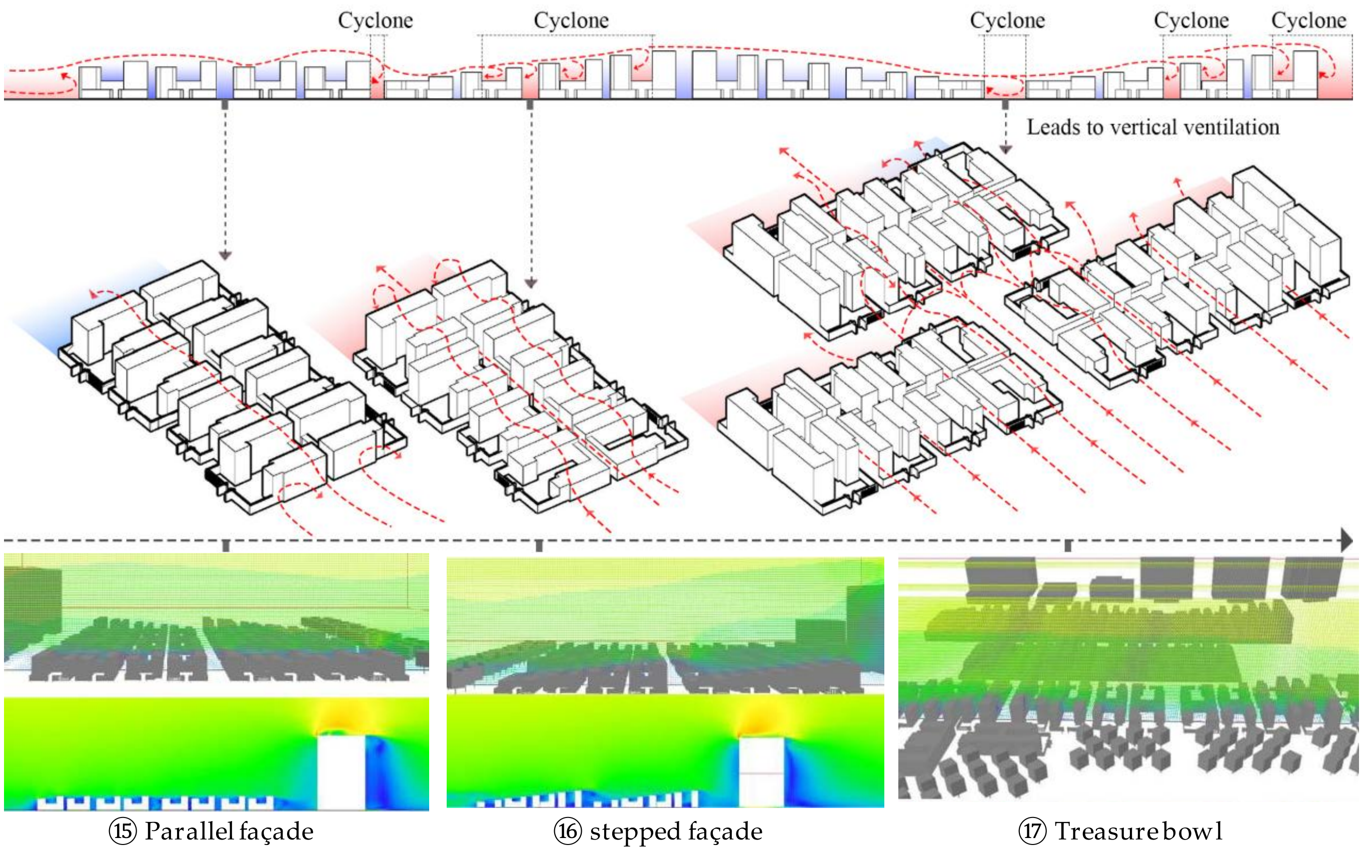

Figure 11. Optimization process of building façade combination and simulation results.

3.2.5. Monolithic Building Openings

Open design is an effective way to increase the air velocity inside a building. The shape and envelope of the building have a substantial effect on the efficiency of natural ventilation [75]. Openings in the building envelope at the front and rear for air entry and discharge can obtain the pressure difference between the front and rear air inlets and outlets, thus promoting natural ventilation. When indoor natural ventilation is generated by outdoor wind pressure, the position of the opening of the building vent relative to the building, and the relative position of the air inlet and outlet of the building, will affect the formation and efficiency of indoor natural ventilation [32]. The above ideas reflect the fact that indoor ventilation is related to the location and scale ratio of the vent openings. To further improve indoor ventilation, the team merged the patio ⑱ and created a concave space to form a canyon effect based on the original layout, and targeted the ventilation openings ⑲ on the side of the wall directly facing the wind direction; see Figure 12 for details of the renovation.

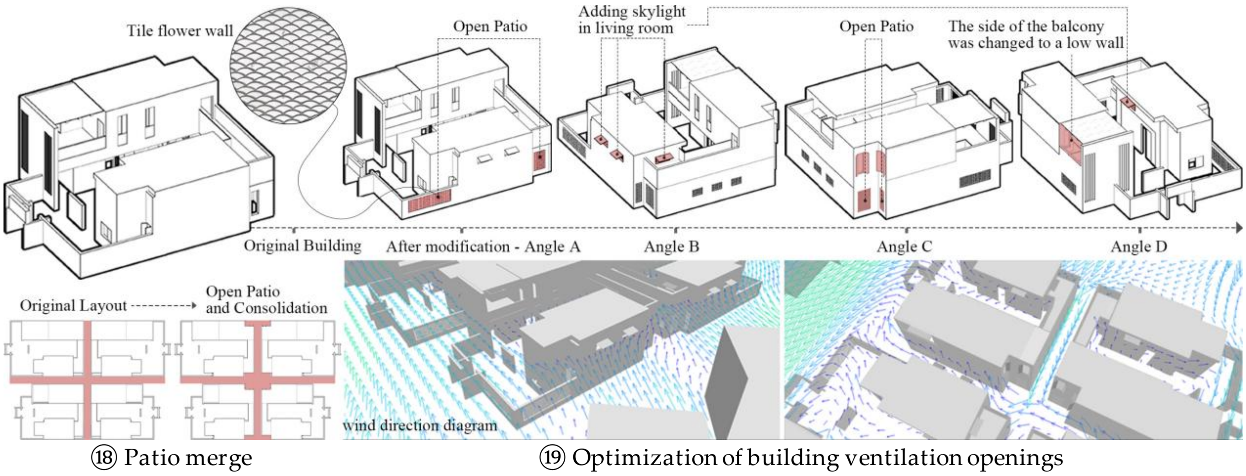

Figure 12. Optimization process of building ventilation openings.

The simulation shows (Figure 13) that the patio merger has little effect on indoor ventilation due to the blockage of the closed exterior wall ⑱, while the high windows opened for ventilation along the side of the wall directly facing the wind can effectively form convective winds with the low windows and the openings of the courtyard's exterior wall, supplementing the courtyard and indoor fresh air ⑲. Further, the tiled wall of the courtyard plays the role of airflow penetration and ensures the role of privacy. Although the wind speed in some indoor spaces still needs to be improved, the interior has basically been transformed from a large area of static wind zone to a quasi-static wind zone, and the wind speed and volume have been effectively improved.

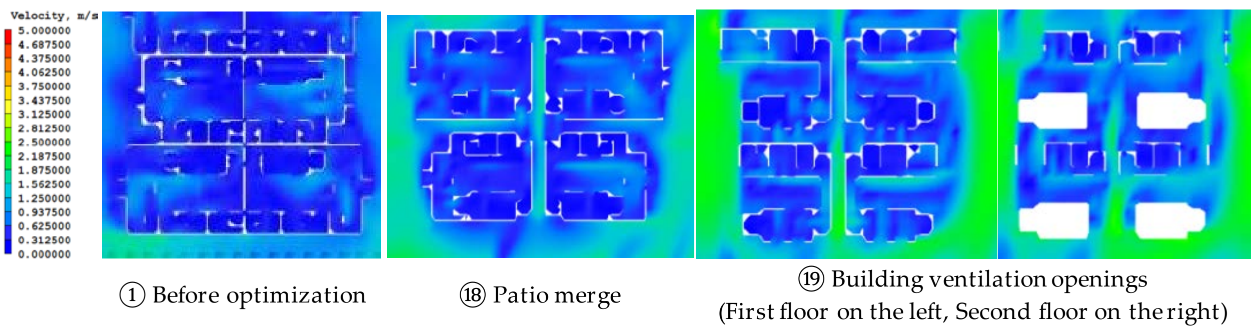

Figure 13. Comparison of simulation for optimization of building ventilation openings.

3.2.6. Indoor Ventilation Block

According to the literature, different window combination designs can effectively improve indoor ventilation [32]. Within a certain scale, when the opening area of the building's air inlet and outlet are equal, the average indoor wind speed is positively correlated with the width of the outlet, and directly related to the width of the vent is the window type and opening method [76], which is related to the external window shape and the area of the window being opened. The four main types of residential villas are casement windows, sliding windows, integrated windows and doors (not open), and fixed windows (not open). When the window-opening area is equal and the window-opening rate is 100%, it is inferred from the research thesis of C.F. Gao [77] of the Hong Kong Polytechnic University that casement windows have better ventilation than sliding windows because sliding windows are fully open and their sash area is only half the size of the window opening. However, real-life experience shows that casement windows are rarely opened at more than a 90° angle, while the area of the sash is equal to the area of the window hole when the center-hung window is fully opened. Even if the window is opened at the same angle as the casement window, it can achieve two-way ventilation on both sides; that is, according to the viewpoint of Ernest D [78] et al. at the University of California, Berkeley: regardless of the angle of the incoming flow, the size of the window opening is proportional to the indoor wind speed, and the indoor wind speed is very closely related to the size of the inlet and outlet and the ratio of its area [79]. Therefore, the team included upper-hung windows, lower-hung windows, longitudinal center-hung windows, and transverse center-hung windows as combination elements, combined with the original windows in the district, to recombine the ventilation modules of each room (Table 10), and calculated the actual window areas N_a' of the modules according to Equation (7) to simulate the effect of the combination of window-opening types and their structures on ventilation. According to the general window-opening behavior of the user, longitudinal center-hung, upper, and lower-hung windows are rarely opened 100%, and this paper sets their N_a' = window-opening area × 30%.

$$N_a' = \text{Fully open window area}/\text{total window} - \text{opening area (openable)} \tag{7}$$

The simulation shows (Figure 14) that, excluding the first-floor guest bedroom and bathroom in the rear building, the wind speed in most of the interior rooms is significantly increased to greater than 0.3 m/s, especially in the second-floor space, where the wind volume is saturated and uniform. Comparing the optimization of the patio ventilation module proves that under the same N_a' condition, the longitudinal center-hung window actually greatly weakens the influence of the opening angle of the window structure on the wind direction due to the advantage of bi-directional air intake during the opening process; the air intake expands with the increase of the opening angle and the ventilation effect is best when opening at an angle of 90°, in contrast to the opening direction and angle of the casement window, which has a greater restriction on the outside air entering the room. Comparing the optimized ventilation module for the master bedroom, it was demonstrated that ventilation through a combination of upper- and lower-hung windows is better than ventilation through a single casement window. Even if only 30% of the upper- and lower-hung windows are opened (N_a' = 0.3), the ventilation effect is still not weaker than opening 100% of the casement windows (N_a' = 1), while the same experimental results are obtained in the comparison of the optimized ventilation module for the second-floor master bathroom. Comparing the guest dining room ventilation module optimization proves that using a combination of longitudinal and transverse center-hung windows for ventilation is better than using a single sliding window for ventilation under the approximate N_a' (0.5→0.63). It is worth mentioning that in this optimization of the guest bedroom ventilation module, even with the expanded N_a' (0.5→0.89) and the combination of lower-hung window ventilation, the ventilation effect of sliding and casement windows is not significantly different, probably because the lower-hung window ventilation needs to reach a certain N_a' in order to fully exploit the effect of airflow exchange.

Table 10. Optimization process of window-opening type combination.

Window type encoding				
	Sliding windows A	Casement windows B	Doors and windows C	Can't open D
	Upper-hung window E	Lower-hung window F	Longitudinally center-hung H	Transverse center-hung G

Ventilation Module (Now)	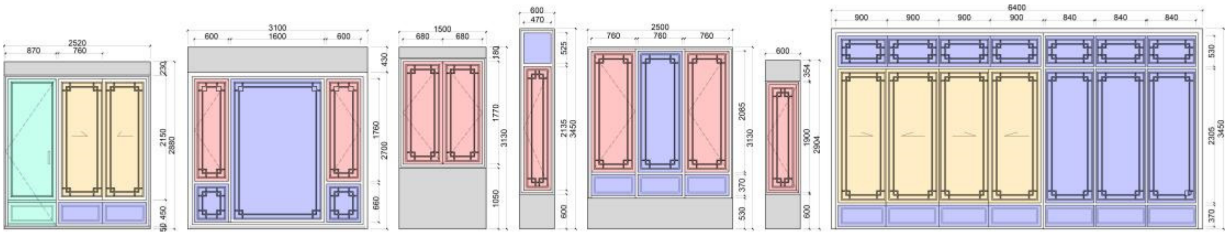						
Area	First-floor bedroom	Master Bedroom second floor	kitchen	Patio	Bathroom on the second floor	Bathroom First floor	The dining room
Combination	1C + 2A + 2D	2B + 3D	2B	1B + 1H	2B + 4D	1B	4A + 17H
N_a'	$\frac{1.58}{3.16} = 0.5$	$\frac{2.07}{2.07} = 1$	$\frac{2.42}{2.42} = 1$	$\frac{1.03}{1.03} = 1$	$\frac{3.17}{3.17} = 1$	$\frac{1.04}{1.04} = 1$	$\frac{4.02}{8.04} = 0.5$
Optimized	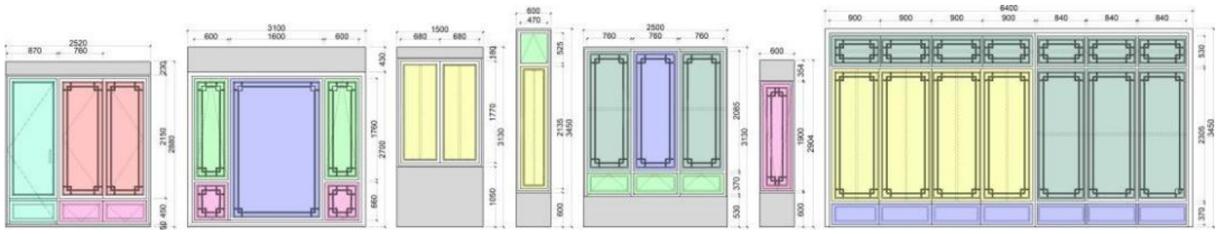						
Combination	1C + 2B + 2D	2E + 2F + 1D	2H	1E + 1H	2G + 3E + 1G	1F	4H + 10G + 7D
N_a'	$\frac{3.32}{3.72} = 0.89$	$\frac{0.85}{2.85} = 0.3$	$\frac{2.42}{2.42} = 1$	$\frac{1.03}{1.03} = 1$	$\frac{1.20}{4.01} = 1$	$\frac{0.31}{1.04} = 0.3$	$\frac{10.7}{16.9} = 0.63$

⑳ Optimized combination of window-opening types

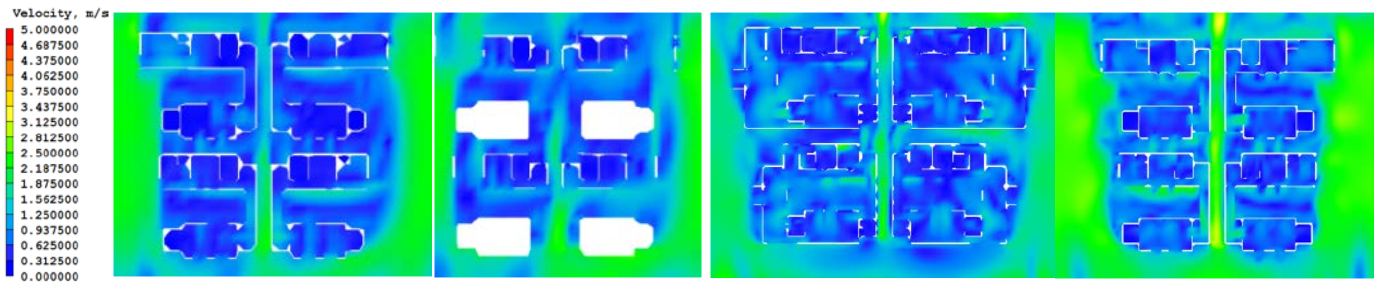

⑲ Building ventilation openings ⑳ Optimized combination of window-opening types

Figure 14. Comparison of simulation for optimization of building ventilation openings.

4. Optimization and Enhancement of Design Strategy Evaluation

The optimization strategy for the wind environment of Moon Island is divided into two aspects: outdoor and indoor. According to the "Beaufort scale" thermal comfort threshold for natural ventilation, the average outdoor wind speed should be no less than 1.6 m/s–3.4 m/s [80]. For indoors, 0.3 m/s–1 m/s [81,82] is the comfortable indoor wind speed in hot and humid areas, while 0.4 m/s is considered to be the effective value to compensate for the evaporative heat and connective tissue heat loss rate of human skin in the environment [83]. In addition, regarding the definition of "static wind zone", 0.1 m/s is defined as the standard of static wind zone [84], but this standard is a strict definition for the atmospheric state, which is relatively low for human comfort and urban pollutant diffusion in building sites. In this study, we took 0.3 m/s as the standard of quasi-static wind zone for evaluation.

Prior to assessment, the various steps of the experimental process were initially coded with serial numbers ranging from 1 to 20, and the wind speed readings were retrieved into an Excel sheet using the PHOENICS software's Probe Location function, and then graphed and totaled using Stata. In Figure 14, the site's average wind speed values can be obtained directly in the GUI Post-Processor (VR Viewer) results panel of PHOENICS. The average wind speed values in the yard for the front and rear rows of buildings are obtained by summing the wind speeds in the yard of all villas in the front or rear rows and then averaging them, and the same principle applies to Figures 15–17.

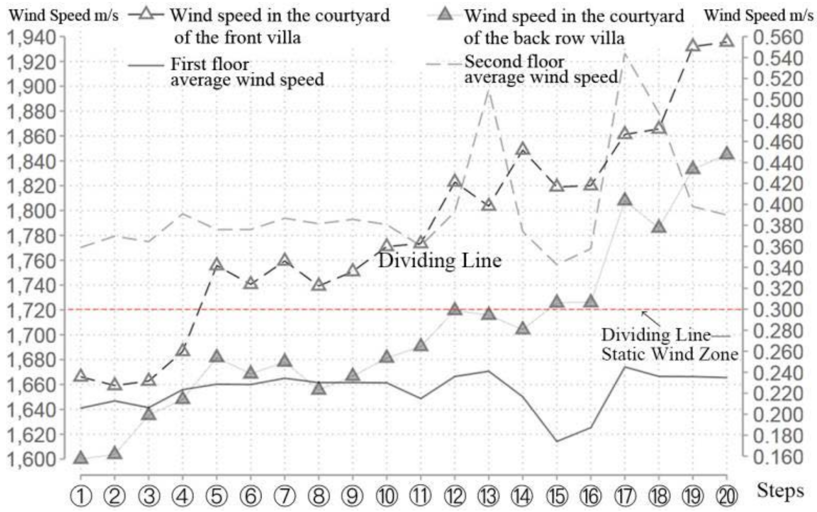

Figure 15. The average outdoor wind speed and the average wind speed in the courtyard of the front and rear buildings at different optimization stages.

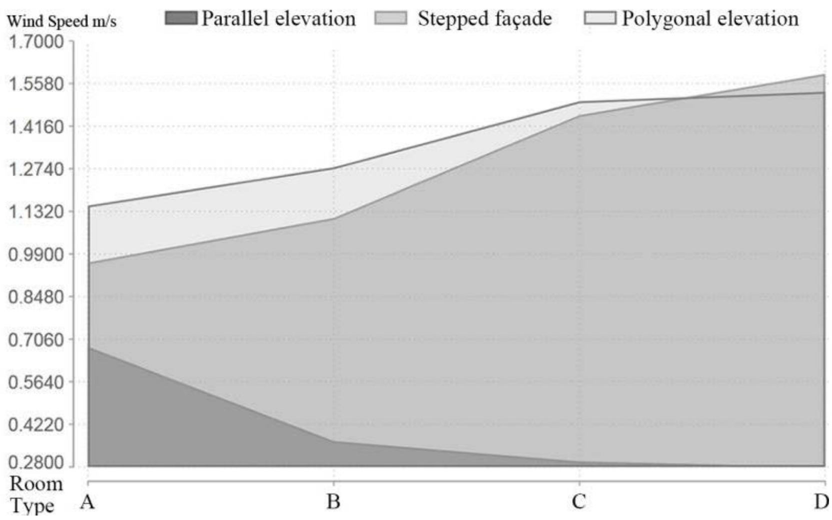

Figure 16. Average wind speed on the windward side of the front and rear rows of buildings with different façade grouping forms.

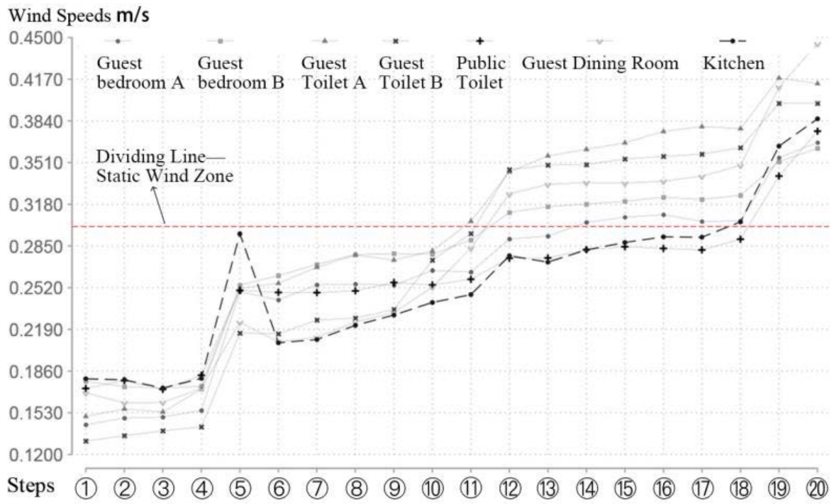

Figure 17. Comparison of average wind speed in the first-floor functional area at different optimization stages.

The previous argumentation process of this study (Table 11) has coded the different optimization processes with ①–⑳. Figure 15 reflects the outdoor simulated wind speed and the in-yard wind speed of the front and back rows of buildings during the comparative optimization process. The figure shows that the average outdoor simulated wind speed values are all greater than 1.6 m/s, which satisfies the comfort value criteria, and the overall outdoor wind speed shows an increasing trend as the optimization progresses. Considering the optimization stages, the average wind speed fluctuates more in the three stages of ⑬, ⑮, and ⑰, which proves that the change of cluster layout has the greatest influence on outdoor wind speed. When the building façade grouping changed from stepped to treasure bowl ⑰, the wind speed in the courtyard of the rear villa increased significantly from 0.306 m/s to 0.403 m/s, proving that the change in height difference between the building façade and the sparse design can effectively improve the ventilation of the rear building. In addition, the wind velocity in the courtyard of the front villa from stage ④ to ⑤ increases significantly from 0.259 m/s to 0.341 m/s, while the wind velocity in the subsequent optimization stage changes slightly. This confirmed that the building orientation has more influence on the outdoor wind velocity than the building group, while the wind velocity from stage ⑱ to ⑲ increases significantly from 0.471 m/s to the level of 0.550 m/s, reflecting that the optimization of building ventilation openings is more effective than building group and façade design for front-row building courtyard ventilation.

Figure 16 reflects the comparison of ventilation under the three façade grouping forms of the building, comparing the change in wind speed on the windward side of the front to the back row of the building (before the wind enters the room), and the lettering from A to D indicates the sequential arrangement from the front to the back row of the house types. The wind velocity area diagram shows that the current parallel façade design of the district greatly hinders the ventilation of the rear-row buildings, while both the stepped and treasure bowl ⑰ designs significantly improve the ventilation of the rear-row house types. When comparing the two, it is obvious that the latter is more effective in taking into account the ventilation of the front-row house types at the same time.

Table 11. The Coding table for improvement steps.

Steps	Adjusted Content	Steps	Adjusted Content
①	Original layout	⑪	Building groups are adjusted to Matrix ventilation + Scale control of cold alley
②	Adjust the roadway scale	⑫	Building groups are adjusted to Fishbone layout
③	Control vegetation density	⑬	Building groups are adjusted to Fishbone style + High-density villas (Vertical)
④	Misplaced layout	⑭	Building groups are adjusted to Fishbone style + High-density villas (Laterally)
⑤	The prevailing wind direction is adjusted to positive southeast	⑮	The façade design of the building group is adjusted to Parallel façade
⑥	The prevailing wind direction is adjusted to positive southwest	⑯	The façade design of the building group is adjusted to stepped façade
⑦	Adjusting the prevailing wind direction to 15° west of south	⑰	The façade design of the building group is adjusted to Treasure bowl
⑧	Building groups are adjusted to One-way ventilation	⑱	Merge Architectural Patio
⑨	Building groups are adjusted to Cross-ventilation	⑲	Optimization of building ventilation openings
⑩	Building groups are adjusted to Matrix ventilation	⑳	Reassembling window-opening types

Figures 17 and 18 compare the wind speed values of each room in different stages. After stage ⑱, excluding the public bathroom, main bathroom, and checkroom, the wind speed values of all rooms are greater than 0.3 m/s, which meets the recommended value of comfortable indoor wind speed. In stages ④→⑤, the wind speed values of all rooms increased significantly, but in stages ⑤→⑥, the wind speed values of the first-floor rooms decreased significantly, reflecting that the indoor ventilation of the first floor was more influenced by the building orientation than that of the second floor. Secondly, in stages ⑪→⑫, the wind speed in all rooms increased to varying degrees (0.205 m/s~0.345 m/s), which proved that the fishbone layout combined with cross-ventilation produced better ventilation effects than simply using matrix ventilation. Then, in stage ⑱→⑲→⑳, excluding the two guest bedrooms on the first floor, wind speed in all other spaces increased to varying degrees (0.29 m/s~0.445 m/s), proving that in addition to changing the orientation, the optimization of building vents and the combination of window types are effective ways to improve indoor ventilation.

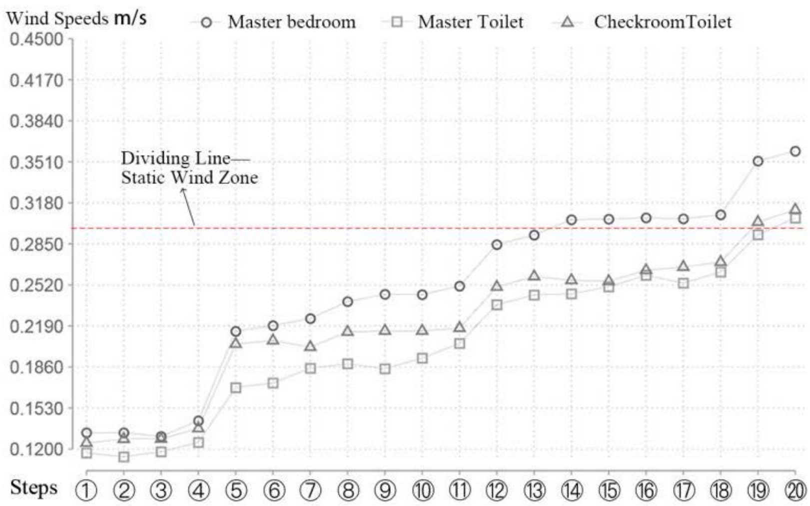

Figure 18. Comparison of average wind speed on the second floor at different optimization stages.

5. Conclusions

This paper compares the effectiveness of natural ventilation under different building forms in the optimization process from cluster to group to single unit. The research process shows that: Building orientation is the most important factor influencing indoor and outdoor ventilation of community villas; factors such as airflow direction, wind angle, building volume and form, and relative position relationship between buildings influence the flow field around buildings; optimization of vents and ventilation modules is one of the key factors in improving indoor ventilation; reasonable design of building façade height difference helps to enhance the ventilation effect.

Conclusions: (1) For the existing villa settlement, the fishbone building layout combined with the staggering green belt is better than the matrix layout in terms of airflow diversion; (2) the best building orientation in the Moon Island district is due southeast, and the best ventilation effect is achieved by the polygon-type façade; (3) the ventilation openings are opened on the side of the direct windward wall, and the combination of various window types is configured according to the characteristics of the outdoor airflow path, which can produce good indoor ventilation; and (4) the "canyon effect" did not achieve the expected effect in this experiment, and the wind speed acceleration effect was reduced when the width of the cold alley exceeded 2 m.

It is clear that the effectiveness of natural ventilation depends on the local climate and the structure's physical characteristics, which are affected by variations in the architectural design. This study validates Cheuk Ming Mak's [58] finding that improved ventilation may be obtained when the angle of wind incidence is 45° from the wall surface and provides case support for the Lingnan region in terms of the influence of building physical parameters on natural ventilation. Additionally, this study compares longitudinal center-hung and transverse center-hung windows to other window types for interior ventilation in the context of combined window-type ventilation, which has received less attention in the past.

Following are some restrictions on the research presented in this paper: (1) In the heat and humidity environment measurement phase, a longer measurement time or comparison of several typical summer days will enhance the study of this work, which is a component that has to be incorporated in future research; (2) in the building façade combination, only the influence of building height difference on fluid is compared; however, the relationship between building and building depth is not compared, due to the need to maintain consistency in the field area size throughout many experimental processes; (3) only two types of merge and open patio are investigated on the impact of airflow during the stage of investigating the monolithic building openings, and the research lacks diversity and hierarchy; (4) indoor layout, door opening direction and location, and material enclosure structure are among the aspects that affect indoor ventilation that are not sufficiently taken into account.

As a result, the goal of our team's upcoming research is to expand the factors affecting a building's natural ventilation to the indoor level and to creatively apply them to local residential architecture and interior design in order to promote the development of a healthy living environment in hot and humid regions.

Author Contributions: Conceptualization, Z.D.; methodology, Z.D. and W.G.; software, W.L.; validation, W.G., W.L., and X.G.; formal analysis, W.L.; investigation, Z.D.; resources, X.G. and W.L.; data curation, X.G.; writing—original draft preparation, W.L. and X.G.; writing—review and editing, Z.D.; visualization, W.L.; supervision, Z.D.; project administration, W.G.; funding acquisition, Z.D. All authors have read and agreed to the published version of the manuscript.

Funding: This research was funded by the Key Project of Humanities and Social Sciences in General Universities of Guangdong Provincial Education Department (Grant no. 2019WZDXM007); Research on the Inheritance and Innovation of Ecological Wisdom of Lingnan Traditional Habitat; the Youth Fund for Humanities and Social Sciences Research of the Ministry of Education (Grant no. 20YJC760135); and Research on the Transmutation of Lingnan Indoor Space Based on Cultural Geography.

Institutional Review Board Statement: Not applicable.

Informed Consent Statement: Not applicable.

Data Availability Statement: Some or all data, models, or code generated or used during the study are available from the corresponding author by request.

Acknowledgments: The authors would like to thank the fund (Grant no. 2019WZDXM007 and 20YJC760135). The author would also like to thank the South China University of Technology Architectural Design and Research Institute platform, and Guo Weihong's team.

Conflicts of Interest: The authors declare no conflict of interest.

References

1. Fan, J.; Zhou, L. Study on the mechanism and effect of urbanization and real estate investment on carbon emissions in China. *Geoscience* **2019**, *39*, 644–653. [CrossRef]
2. Deng, L. Analysis of the competitiveness of export industries in the Pearl River Delta. *Special Economic Zone* **2010**, *9*, 27–28.
3. Yang, C. Evening News: Guangzhou's Social Electricity Consumption and Power Supply both Exceeded 100 Billion kwh. Available online: https://m.gmw.cn/baijia/2021-12/14/1302720245.html (accessed on 21 July 2022).
4. Omer, A.M. Renewable building energy systems and passive human comfort solutions. *Renew. Sustain. Energy Rev.* **2008**, *12*, 1562–1587. [CrossRef]
5. Li, B.; Guo, W.; Dou, J.; Liu, S.; Zhang, Y. Study on thermal environment diagnosis and treatment from the perspective of healthy habitat. *Ind. Archit.* **2021**, *51*, 19–27. [CrossRef]
6. Knowing: A look at the Relationship between Real Estate and GDP, Population, and Urbanization. Available online: https://zhuanlan.zhihu.com/p/25487755?utm_source=wechat_session&utm_medium=social&utm_oi=956465185184075776&utm_campaign=shareopn (accessed on 21 July 2022).
7. Stabile, L.; Dell'Isola, M.; Frattolillo, A.; Massimo, A.; Russi, A. Effect of natural ventilation and manual airing on indoor air quality in naturally ventilated Italian classrooms. *Build. Environ.* **2016**, *98*, 180–189. [CrossRef]
8. Wang, B.; Malkawi, A. Design-based natural ventilation evaluation in early stage for high performance buildings. *Sustain. Cities Soc.* **2019**, *45*, 25–37. [CrossRef]
9. Omrani, S.; Garcia-Hansen, V.; Capra, B.; Drogemuller, R. Natural ventilation in multi-storey buildings: Design process and review of evaluation tools. *Build. Environ.* **2017**, *116*, 182–194. [CrossRef]
10. Masoumi, H.R.; Nejati, N.; Ahadi, A. Learning from the heritage architecture: Developing natural ventilation in compact urban form in hot-humid climate: Case study of Bushehr, Iran. *Int. J. Archit. Herit.* **2017**, *11*, 415–432. [CrossRef]
11. Guo, W.; Li, B.; Dou, J.; Zhang, Z. Research on the wind environment design of healthy settlements based on epidemic prevention—an example of Lingnan Moon Island settlement. *South. Archit.* **2020**, *4*, 14–21. [CrossRef]
12. Guo, W.; Liu, X.; Yuan, X. Research on optimal design of natural ventilation in green buildings based on CFD simulation. *Build. Build. Energy Effic.* **2015**, *43*, 45–52.
13. Reardon, C.; Milne, G.; McGee, C. *Your Home Technical Manual*; Australian Government Department of Climate Change and Energy Efficiency: Canberra, Australia, 2010.
14. Cui, K. My View of Green Building [EB/OL]. 2016. Available online: https://huanbao.bjx.com.cn/news/20161226/799487-2.shtml?txxxbs=sogou (accessed on 21 July 2022).
15. Olgyay, V. *Design with Climate: Bio-Climatic Approach to Architectural Regionalism*; Princeton University Press: Princeton, NJ, USA, 1963.
16. Correa, C.M. *Form follows climate*; World Microfilms Publications Ltd.: London, UK, 1980.
17. Wang, F. *Charles Coria*; China Construction Industry Press: Beijing, China, 2003.
18. Xiao, Y.; Wang, J.; Qi, B. Consideration of heat protection mode of building exterior skin under humid and hot climate. *South. Archit.* **2010**, *1*, 60–63.
19. Mo, B. The planning and construction of residential buildings in Guangzhou. *J. Archit.* **1959**, *1*, 21–25.
20. Lin, Q. On the improvement of the habitat of Lingnan buildings and building energy conservation. *J. South China Univ. Technol.* **1997**, *1*, 48–52.
21. Gideon, S.; Golany, Z.Z. *Environmental Ethics of Urban Design*; Liaoning People's Publishing House: Shenyang, China, 1995.
22. Xiao, Y.; Feng, J. The formation and development of architectural education and creative thought in the School of Architecture of South China University of Technology. *South. Archit.* **2008**, *1*, 23–27.
23. Lin, X. *Green Architectural Design for Hot and Humid Climates: From Ecological Architecture to Global Environmental Protection*; Zhangshi Books: Taipei, Taiwan, 1996; p. 103.
24. Gao, Y.; Qinglin, M. An ecological building technology—Natural ventilation. *Ecol. Sci.* **2003**, *1*, 86–89.
25. Xie, H. Natural Ventilation of Lingnan Houses. *Small Town Constr.* **2007**, 58–62.
26. Hui, X. *Study on climate adaptation of spatial system of cold lane courtyard in traditional village in Guangfu area*; South China University of Technology: Guangzhou, China, 2016.

27. Xiao, Y.; Liu, S. A study on the scale of traditional architectural climate space in Lingnan. *Dyn. Ecol. Cities Green Build.* **2015**, 73–79.
28. Song, D. *Energy efficient building design and technology*; Tongji University Press: Shanghai, China, 2003.
29. Mai, H. *Research on Climate Adaptation Creation Strategy of Contemporary Lingnan Architecture Based on Holistic View*; South China University of Technology: Guangzhou, China, 2016.
30. Zeng, Z. *Ventilation Methods for Traditional Houses in Guangfu and Their Modern Architectural Applications*; South China University of Technology: Guangzhou, China, 2010.
31. Yang, A.S.; Wen, C.Y.; Juan, Y.H.; Su, Y.-M.; Wu, J.H. Using the central ventilation shaft design within public buildings for natural aeration enhancement. *Appl. Therm. Eng.* **2014**, *70*, 219–230. [CrossRef]
32. Fang, P. *Research on the Influence of the Design form of High-Rise Residential Exterior Windows on Indoor Natural Ventilation*; Hefei University of Technology: Guangzhou, China, 2018.
33. Xia, Y. *Ecological and Sustainable Architecture*; China Construction Industry Press: Beijing, China, 2001; p. 6.
34. Li, B.; Guo, W.; Liu, X.; Zhang, Y.; Russell, P.J.; Schnabel, M. Sustainable Passive Design for Building Performance of Healthy Built Environment in the Lingnan Area. *Sustainability* **2021**, *13*, 9115. [CrossRef]
35. Nie, J.; Pang, Y.; Wang, C.; Zhang, H.; Tin, K. Theoretical Study on the Relationship of Building Thermal Insulation with Indoor Thermal Comfort Based on APMV Index and Energy Consumption of Rural Residential Buildings. *Appl. Sci.* **2021**, *11*, 8565. [CrossRef]
36. *GB/T 18049-2017*; Ergonomics of Thermal Environments Analytical Determination and Interpretation of Thermal Comfort by Calculating PMV and PPD Indices with Local Thermal Comfort Guidelines. ISO: Geneva, Switzerland, 2017.
37. *JGJ/T 347-2014*; Standard on Test Methods for the Thermal Environment of Buildings. ISO: Geneva, Switzerland, 2014.
38. *GB/T 50785-2012*; Evaluation Standard for Indoor Thermal and Humid Environment in Civil Buildings. ISO: Geneva, Switzerland, 2012.
39. Zhu, Y. *Built Environment*; China Construction Industry Press: Beijing, China, 2010.
40. Orosa, J.A.; Oliveira, A.C. A new thermal comfort approach comparing adaptive and PMV models. *Renew. Energy* **2011**, *36*, 951–956. [CrossRef]
41. *GB/T 50378-2014*; Green Building Evaluation Standard. Article 4.1.12 General Items. ISO: Geneva, Switzerland, 2014.
42. Yang, L. *Building Climatology*; China Construction Industry Press: Beijing, China, 2010.
43. *JGJ/T 449-2018*; Green Performance Calculation Standard for Civil Buildings. Appendix B. ISO: Geneva, Switzerland, 2018.
44. De Dear, R.; Brager, G.S. Developing an adaptive model of thermal comfort and preference. *ASHRAE Trans.* **1998**, *97*, 874–879.
45. Wolkoff, P.; Kjærgaard, S.K. The dichotomy of relative humidity on indoor air quality. *Environ. Int.* **2007**, *33*, 850–857. [CrossRef] [PubMed]
46. Kubota, T.; Hooi Chyee, D.T. Potential of passive cooling techniques for modern houses in the tropical climate of Malaysia–analysis of the indoor thermal environment for various ventilation strategies. *Int. J. Vent.* **2010**, *9*, 11–23. [CrossRef]
47. Michael, A.; Demosthenous, D.; Philokyprou, M. Natural ventilation for cooling in mediterranean climate: A case study in vernacular architecture of Cyprus. *Energy Build.* **2017**, *144*, 333–345. [CrossRef]
48. Guo, W.; Liu, X.; Yuan, X. Study on natural ventilation design optimization based on CFD simulation for green buildings. *Procedia Eng.* **2015**, *121*, 573–581. [CrossRef]
49. Cheng, J. *CFD-Based Numerical Simulation of Flow Field and Air Pollution in Residential Communities*; Fudan University: Shanghai, China, 2012.
50. Yang, L.; Liu, X.; Qian, F.; Du, S. Ventilation effect on different position of classrooms in "line" type teaching building. *J. Clean. Prod.* **2019**, *209*, 886–902. [CrossRef]
51. Guo, W.H.; Liu, X.; Yuan, X. A case study on optimization of building design based on CFD simulation technology of wind environment. *Procedia Eng.* **2015**, *121*, 225–231. [CrossRef]
52. Li, B.; Guo, W.; Schnabel, M.A. Feng-Shui and Computational Fluid Dynamics (CFD)-Analyzing Natural Ventilation and Human Comfort. In Proceedings of the 25th International Conference of the Association for Computer-Aided Architectural Design Research in Asia, Bangkok, Thailand, 5–6 August 2020; Association for Computer-Aided Architectural Design Research in Asia: Hong Kong, China.
53. Mochida, A.; Yoshino, H.; Takeda, T.; Kakegawa, T.; Miyauchi, S. Methods for controlling airflow in and around a building under cross-ventilation to improve indoor thermal comfort. *J. Wind. Eng. Ind. Aerodyn.* **2005**, *93*, 437–449. [CrossRef]
54. Lechner, N. *Heating, Cooling, Lighting: Sustainable Design Methods for Architects*; John Wiley & Sons: Hoboken, NJ, USA, 2014.
55. Aflaki, A.; Mahyuddin, N.; Mahmoud, Z.A.C.; Baharum, M.R. A review on natural ventilation applications through building façade components and ventilation openings in tropical climates. *Energy Build.* **2015**, *101*, 153–162. [CrossRef]
56. Liping, W.; Hien, W.N. The impacts of ventilation strategies and facade on indoor thermal environment for naturally ventilated residential buildings in Singapore. *Build. Environ.* **2007**, *42*, 4006–4015. [CrossRef]
57. Haase, M.; Amato, A. An investigation of the potential for natural ventilation and building orientation to achieve thermal comfort in warm and humid climates. *Sol. Energy* **2009**, *83*, 389–399. [CrossRef]
58. Mak, C.M.; Niu, J.L.; Lee, C.T.; Chan, K.F. A numerical simulation of wing walls using computational fluid dynamics. *Energy Build.* **2007**, *39*, 995–1002. [CrossRef]

59. Yani, Z.; Nigang, H.; Shi, Y.; Yiqiang, X. Research on the evaluation of urban design elements in humid and hot areas based on wind-heat environment optimization—A case study of Baiyun New Town in Guangzhou. *J. Urban Plan.* **2019**, 109–118.
60. Kumar, N.; Kubota, T.; Tominaga, Y.; Shirzadi, M.; Bardhan, R. CFD simulations of wind-induced ventilation in apartment buildings with vertical voids: Effects of pilotis and wind fin on ventilation performance. *Build. Environ.* **2021**, *194*, 107666. [CrossRef]
61. Ramponi, R.; Blocken, B.; Laura, B.; Janssen, W.D. CFD simulation of outdoor ventilation of generic urban configurations with different urban densities and equal and unequal street widths. *Build. Environ.* **2015**, *92*, 152–166. [CrossRef]
62. Yang, L.; Liu, X.; Qian, F.; Niu, S. Research on the wind environment and air quality of parallel courtyards in a university campus. *Sustain. Cities Soc.* **2020**, *56*, 102019. [CrossRef]
63. Wu, J. *Analysis of the Spatial Organization Characteristics and Technical Treatment of Vernacular Architecture in Southern Jinan*; Taiyuan University of Technology: Taiyuan, China, 2010.
64. Wei, Q.; Zhijia, H.; Lingling, Z.; Tuantuan, S. Research on natural ventilation creation technology of traditional residential houses in southern Anhui. *J. Anhui Univ. Technol. (Nat. Sci. Ed.)* **2013**, *30*, 261–265.
65. Ye, Q. *Research on Suitable Wind Environment-Oriented Outdoor Space Design for Residential Areas in Guangzhou*; Guangzhou University: Guangzhou, China, 2017.
66. Liu, J. *Research on the Characteristics and Optimization Strategies of Wind Environment Impact on Multi-Storey Settlements in Cold High-Rise Settlements*; Tianjin University: Tianjin, China, 2017.
67. Mumovic, D.; Santamouris, M. *A Handbook of Sustainable Building Design and Engineering: An Integrated Approach to Energy, Health and Operational Performance*; Routledge: London, UK, 2013.
68. Zhao, H. *The Relationship between Natural Ventilation and Indoor air Quality and Thermal Environment of Residential Buildings—A Case Study of Residential Buildings in Beijing*; Beijing Institute of Construction Engineering: Beijing, China, 2007.
69. Wang, J. *Research on Wind Environment Improvement Strategies for Residential Compounds in Villages and Towns in the Severe Cold Region of Northeast China*; Harbin Institute of Technology: Harbin, China, 2015.
70. Klote, J.H. *A General Routine for Analysis of Stack Effect*; National Institute of Standards and Technology: Gaithersburg, MD, USA, 1991.
71. Zheng, Z.; Chen, L.; Yang, R. Occupation and enclosure of architectural space forms. *Sichuan Archit. Sci. Res.* **2008**, *34*, 217–219.
72. Liping, W.; Hien, W.N. Applying natural ventilation for thermal comfort in residential buildings in Singapore. *Archit. Sci. Rev.* **2007**, *50*, 224–233.
73. Li, Y. *The Reality of Living in China and the Design of Well-Off Houses*; Southeast University Press: Nanjing, China, 1999.
74. Zhengrong, L.; Zhengtao, A. Numerical study on the effect of balconies on natural ventilation under wind pressure in low-rise buildings. *Build. Sci.* **2011**, *27*, 87–91.
75. Chou, P.C.; Chiang, C.M.; Li, Y.Y.; Lee, C.-Y.; Chang, K.-F. Natural ventilation efficiency in a bedroom with a central-pivoting window. *Indoor Built Environ.* **2008**, *17*, 164–172. [CrossRef]
76. Fung, Y.W.; Lee, W.L. Identifying the most influential parameter affecting natural ventilation performance in high-rise high-density residential buildings. *Indoor Built Environ.* **2015**, *24*, 803–812. [CrossRef]
77. Gao, C.F.; Lee, W.L. Evaluating the influence of openings configuration on natural ventilation performance of residential units in Hong Kong. *Build. Environ.* **2011**, *46*, 961–969. [CrossRef]
78. Ernest, D.; Bauman, F.; Arens, E.A. The prediction of indoor air motion for occupant cooling in naturally ventilated buildings. *ASHRAE Trans.* **1991**, *97*, 1.
79. Wu, D. *Research on the Influence of Design Style of High-Rise Residential Exterior Windows on Indoor Natural Ventilation*; Beijing University of Architecture: Beijing, China, 2014.
80. Cheng, V.; Ng, E. Thermal comfort in urban open spaces for Hong Kong. *Archit. Sci. Rev.* **2006**, *49*, 236–242. [CrossRef]
81. Cândido, C.; de Dear, R.; Lamberts, R. Combined thermal acceptability and air movement assessments in a hot humid climate. *Build. Environ.* **2011**, *46*, 379–385. [CrossRef]
82. *CJJ/T 309-2013*; Building Ventilation Effect Testing and Evaluation Standards. ISO: Geneva, Switzerland, 2013.
83. Tantasavasdi, C.; Srebric, J.; Chen, Q. Natural ventilation design for houses in Thailand. *Energy Build.* **2001**, *33*, 815–824. [CrossRef]
84. General Administration of Quality Supervision, Inspection and Quarantine, National Standardization Administration. *Tropical Cyclone Classification: GB/T 19201-2006*; Commercial Press: Beijing, China, 2006; p. 9.